NATIONAL ADVISORY COMMITTEE FOR AERONAUTICS

WARTIME REPORT

ORIGINALLY ISSUED

December 1944 as
Memorandum Report A4L18

HIGH-SPEED WIND-TUNNEL TESTS OF SEMISPAN HORIZONTAL TAILS WITH FABRIC-COVERED AND METAL-COVERED ELEVATORS FOR A BOMBER AIRPLANE

By Albert L. Erickson and Warren H. Nelson

Ames Aeronautical Laboratory
Moffett Field, California

NACA

WASHINGTON

MR No. A4L18

NATIONAL ADVISORY COMMITTEE FOR AERONAUTICS

MEMORANDUM REPORT

for the

Air Technical Service Command, U.S. Army Air Forces

HIGH-SPEED WIND-TUNNEL TESTS OF SEMISPAN HORIZONTAL TAILS WITH FABRIC-COVERED AND METAL-COVERED ELEVATORS FOR A BOMBER AIRPLANE

By Albert L. Erickson and Warren H. Nelson

SUMMARY

This report contains the results of tests of a full-scale semispan horizontal tail plane of a bomber airplane. The effects of fabric distortion on the aerodynamic characteristics of the elevator are determined by comparing the aerodynamic characteristics of a fabric-covered elevator with those of a metal-covered elevator. In addition, the results of cutting holes in the balance seal, the effect of fixing transition, the tab effectiveness both sealed and unsealed, and the section drag of this tail plane are presented.

The results of the tests show that fabric deformation can cause extreme changes in stick force at high speed. At 0.72 Mach number, the calculated stick force per unit normal acceleration for the fabric-covered elevator was three times the force for the metal-covered elevator. It is also shown that the tab effectiveness can be trebled by sealing the gap at the leading edge of the tab.

INTRODUCTION

The increasing speed and size of airplanes have caused the design of control surfaces to become extremely critical. At the highest speeds, because of the close balance required, a slight variation in the control contour can cause extreme changes in the control forces.

There have been numerous cases where flight data have shown the rather serious effects of fabric distortion. Reference 1 discussed several of these cases in which very large stick forces that occurred in flight were found to be caused by fabric distortion. The qualitative effects of slight changes in contour, such as might be caused by fabric distortion, are given in references 2, 3, and 4. Reference 2 is an analytical study of the stick forces that would result from various types of fabric distortion, and shows that fabric distortion can cause extreme changes in the control characteristics.

The tests discussed in this report were initiated to determine the effects of distortion of the fabric covering of the bomber elevator at high speeds. Quantitative results on the effect of fabric distortion by direct comparisons of the characteristics of a metal-covered elevator with those of a fabric-covered elevator are included. In addition, the effects of installing leak holes in the elevator balance seal, sealing the tab, and fixing transition on the stabilizer are presented. The results of measurement of the sectional drag coefficient of this production-type low-drag tail plane are also included.

The data were obtained in the 16-foot high-speed wind tunnel at the Ames Aeronautical Laboratory, Moffett Field, Calif.

SYMBOLS

Standard NACA symbols and coefficients used throughout the report are defined as follows:

α airplane angle of attack, degrees (angle measured from fuselage reference line)

α_t angle of attack of horizontal tail, degrees (zero lift occurred at -1.89°)

δ_e elevator angle, degrees

δ_t tab angle, degrees

M Mach number

c_{d_o}	airfoil section drag coefficient
C_{h_e}	elevator hinge-moment coefficient ($H_e/qb_e\overline{c}^2$)
H_e	elevator hinge moment, foot-pounds
q	dynamic pressure ($\frac{1}{2}\rho V^2$), pounds per square foot
b_e	elevator span, feet
$\overline{c}$	root-mean-square chord of elevator behind hinge line, feet
C_{L_t}	lift coefficient of tail (L_t/qS_t)
L_t	lift of tail, pounds
S_t	area of tail, square feet
C_{m_t}	pitching-moment coefficient due to tail [$M_t/qS_w(M.A.C.)_w$]
M_t	moment about the center of gravity due to the tail, foot-pounds
S_w	area of wing, square feet
$M.A.C._H$	mean aerodynamic chord of horizontal tail
$M.A.C._w$	mean aerodynamic chord of airplane wing
P	pressure coefficient $(p - p_o)/q$
p	local static pressure, pounds per square foot
p_o	free-stream static pressure, pounds per square foot
P_{cr}	critical pressure coefficient

APPARATUS AND METHODS

A full-scale semispan horizontal tail plane from the bomber airplane was used for these tests. A stub section was provided so that the tunnel wall was at the position

corresponding to the airplane center line (fig. 1). There was a gap of approximately 3/16 inch between the model and the tunnel wall, but it was found that this gap had no measurable effect on the elevator hinge moments. The tail plane was mounted upside down in the tunnel. The streamline tie rod, shown in figure 1, was used to increase the allowable negative lift loads. The model was supported by the balance frame so that all forces and moments could be measured by the six-component scale system.

The elevator angle was controlled by an electric motor, and maintained at a constant setting by an automatic positioning device. Hinge moments were measured with a calibrated electric strain gage mounted on a special arm in the elevator control linkage.

The general dimensions and plan view of the tail plane as tested are shown in figure 2. Figure 3 shows a sectional drawing of the stabilizer, elevator, and tab. Figure 4 shows the rib spacing in the elevator, and gives the specifications for the fabric covering and its application.

ANALYSIS OF DATA

The data have been corrected for tunnel-wall effects. The correction varied across the span of the wing; however, a weighted-average correction to the angle of attack, equal to 0.898 C_L, was added. The data also have been corrected for the effects of constriction on the dynamic pressure and Mach number.

Wherever slopes are given in the text they refer to the slope through zero stabilizer angle, elevator angle, or tab angle, as the case may be.

In analyzing the data, stick forces were computed for three Mach numbers. It was necessary to compute these stick forces for fictitious conditions, because the strength of the support system was such that it was not possible to attain stabilizer and elevator angles that would completely correspond to those of the bomber airplane at high speed. In order to use the data obtained to the best advantage for comparative purposes, the following conditions were used in the calculations:

(a) The stabilizer was set at 1° angle of incidence. (It is at 0° on the airplane.)

(b) The downwash at the tail was computed as being equal to 5.2 C_{L_w}.

(c) Tail-off pitching moments from the 17.5-percent scale model of the bomber airplane tested in the 16-foot wind tunnel were used (reference 5).

(d) Because data at only one stabilizer angle were obtained at high speed during the model tests, no correction to $\partial C_{m_t}/\partial \alpha_t$ for fuselage interference was possible. This effect would not change the differences between the characteristics calculated for the fabric-covered and metal-covered surfaces.

(e) The stabilizer angle and elevator angles used for the comparative stick forces shown for a Mach number of 0.133 were obtained from tests of a model of the bomber airplane in the 7- by 10-foot wind tunnel.

RESULTS AND DISCUSSION

Comparison of Fabric-Covered and Metal-Covered Elevators

At a Mach number of 0.133 there was no noticeable distortion of either elevator. Figures 5 to 8 show that, as would be expected, the fabric-covered and metal-covered elevators had similar aerodynamic characteristics at this low Mach number.

At a Mach number of 0.33, the fabric surface began to show slight distortions; for an elevator angle of 0° the slope $\partial C_{h_e}/\partial \alpha_t$ is -0.0009 for the fabric-covered elevator and 0.0005 for the metal-covered elevator (figs. 9(a) and 9(b)). The tail effectiveness $\partial C_{m_t}/\partial \alpha_t$ remains practically the same for the two elevators (figs. 10 (a) and 10 (b)). The slope $-\partial C_{h_e}/\partial \delta_e$ is about 50 percent greater for the fabric-covered elevator (fig. 11). The comparative stick forces in figure 12 show a slightly greater variation of stick force with center-of-gravity position for the fabric-covered elevator. The computed stick-force variation with indicated acceleration is

the same for both elevators (fig. 13). It is to be noted in both figures 12 and 13 that the principal effect of fabric distortion at this speed would be to change the airplane trim.

The deformations of the fabric-covered and metal-covered elevators at 0.72 Mach number are shown in figures 14 and 15. These figures show that the fabric was distorted to a concave shape on both the upper and lower surfaces, as was true under all conditions tested. In figure 15 it is seen that the metal surface was slightly distorted so that its characteristics are not those of a rigid surface. From these pictures it should be recognized that the differences shown in comparing the fabric surface with the metal surface are not as large as the differences between the fabric-covered elevator and a rigid-surface elevator.

At 0.72 Mach number an extremely large change is effected in the comparative aerodynamic characteristics of the fabric-covered and metal-covered elevators. Although the data at 0.72 Mach number were limited by the model strength, the large differences are clearly evident (figs. 16 to 22). In figures 16(a) and 16(b), $\partial C_{h_e}/\partial \alpha_t$ is 0.0020 for the metal-covered elevator and -0.0010 for the fabric-covered elevator. The curves of $\partial C_{h_e}/\partial \alpha_t$ for the metal-covered elevator have a discontinuity between -2° and -2.3° angle of attack, which is probably due to separation caused by supercritical speeds. Figure 17 shows an extreme difference in $\partial C_{h_e}/\partial \delta_e$. This slope is -0.0038 for the fabric surface and -0.0005 for the metal surface. The small value of $-\partial C_{h_e}/\partial \delta_e$ for the metal-covered elevator at 0.72 Mach number (fig. 17) was determined from a very limited amount of data. Since the elevator profile has but slight effect on $-\partial C_{h_e}/\partial \delta_e$ at large elevator angles, this slope would probably assume a value similar to that for the fabric-covered elevator at larger negative and positive elevator angles. Figures 18(a) and 18(b) show that the tail effectiveness $\partial C_{m_t}/\partial \alpha_t$ remains the same for both elevators. The effect of the distortion of the fabric surface on the various parameters is to be expected, and probably could be predicted if the exact distortion were known (references 2 and 3).

Stick forces computed for 0.72 Mach number are presented in figures 19(a) and 19(b). The stick force per g is 60 pounds for the fabric-covered elevator and only 20 pounds for the metal-covered elevator. The results show that it would be impossible to predict control forces accurately from model

data if the airplane has control surfaces that distort.

Because of the importance of the trailing-edge angle in determining elevator characteristics (references 3 and 6), it is believed that if the aft 5 or 10 percent of the elevator were made of metal and the surface vented at the trailing edge, the stick forces would more nearly compare with results predicted from tests of rigid control surfaces.

Figures 20 and 21 show the pressure distribution over the lower surface of the stabilizer at 0.33 and 0.72 Mach numbers. In figure 21(b) a slight difference in the pressures near the peak is noted, the stabilizer with the fabric-covered elevator having slightly higher local velocities. Pressures over the elevator were not measured; however, balance-well pressures were measured, and it is shown in figure 22 that the balancing hinge moments computed from the balance-well pressures are not appreciably affected by the elevator contour changes. Therefore, the large changes in elevator hinge moments are almost entirely due to the changes aft of the elevator hinge line.

Figures 23(a), 23(b), 24, and 25 show the condition of the fabric surface before and after running at high speed. The looseness of the fabric after a run at high speed depended on humidity, temperature, and length of time at high-speed conditions. Under static conditions the fabric gradually became taut again.

Effects of Leak Holes in the Balance Seal

Sixteen holes, 1-1/16 inches in diameter, were cut in the balance seal, as noted in figure 3. The effects of these openings are presented in figures 26 to 32. The slope $-\partial C_{h_e}/\partial \alpha_t$ was not changed by the leak holes, but the slope $-\partial C_{h_e}/\partial \delta_e$ was about doubled. The calculated stick force per g at 0.33 Mach number for sea-level conditions is about 13 pounds with the sealed balance and about 26 pounds with the holes in the seal. In general, the stick-force gradients are about doubled when the leak holes are placed in the balance seal.

Tab Effectiveness

The tab effectiveness $-\partial C_{h_e}/\partial \delta_t$ is about 0.0035 at both 0.133 and 0.33 Mach numbers (figs. 33 and 34). At 0.72 Mach number the effectiveness drops off slightly to 0.0025 (fig. 35). In order to increase the tab effectiveness, the gap at the leading edge of the tab was sealed as indicated in figure 3. The effectiveness at 0.72 Mach number increased to about 0.0072 (fig. 35). At sea level and 0.72 Mach number the stick force per degree tab angle is about 42 pounds for the unsealed tab and about 110 pounds for the sealed tab. The stick forces per degree tab angle at 20,000 feet altitude are 16 pounds for the unsealed tab and about 56 pounds for the sealed tab (fig. 36). Data at 0.72 Mach number were taken at only two tab angles ($\pm 1^\circ$) and were taken as near the same time as possible so that the fabric tautness would be constant.

Effect of Fixed Transition

The breaks in $\partial C_{h_e}/\partial \alpha_t$ and $\partial C_{m_t}/\partial \alpha_t$, noted in figures 5(a) and 6(a), were believed to be caused by a sudden forward movement of the transition point. Transition was fixed at 20 percent chord by means of a strip of carborundum in order to investigate this effect, and the results are shown in figures 37 and 38. These results show that there were no breaks in the curves (fig. 38) when the transition point was fixed, hence the breaks that occurred when the point of transition was not fixed were probably caused by a forward movement of the transition point. Figure 39 shows that, at an elevator angle of -20°, the pressure distribution on the stabilizer with the fabric-covered elevator changes from a favorable gradient at 4° angle of attack to an unfavorable gradient at -4°. Transition would be expected to occur at about 0° or at a slightly more negative angle, which would agree with the transition breaks noted on the curves (figs. 37 and 38). The breaks noted in these data are probably not as sharp on the airplane due to the interference of the fuselage. The turbulence level of the 16-foot wind tunnel is very low, and probably the effective Reynolds number in the tunnel closely approximates that at the tail of the airplane in free air.

Section Drag

The section drag of the bomber horizontal tail was measured by the momentum method, and the results are presented

in figures 40 and 41. The surface was not prepared specially, except that all obvious rough spots were lightly sanded. A two-dimensional smooth model of this stabilizer and elevator was tested in the Langley two-dimensional wind tunnel, where the lowest section drag obtained was about 0.0045. Compared to this value, the production tail plane in the 16-foot high-speed wind tunnel at the Ames Laboratory had a minimum section drag of about 0.0052 at one station. The momentum-drag measurements are of questionable accuracy because of the spanwise flow on the three-dimensional body.

CONCLUDING REMARKS

At 0.72 Mach number, the stick force per unit normal acceleration calculated from the test results for the fabric-covered elevator was three times the force for the metal-covered elevator. This large difference indicates serious aerodynamic design difficulties if fabric-covered elevators are used.

The metal covering also distorted slightly (fig. 15(b)); therefore, when designing this type of surface the distortion must be considered.

It is indicated that, at the two tab angles tested, sealing the gap at the leading edge of the tab triples the tab effectiveness.

Ames Aeronautical Laboratory,
National Advisory Committee for Aeronautics,
Moffett Field, Calif.

REFERENCES

1. Phillips, W. H.: Effects of Fabric Deflection on Control Characteristics. NACA RB, Mar. 1943.

2. Mathews, Charles W.: An Analytical Investigation of the Effects of Elevator-Fabric Distortion on the Longitudinal Stability and Control of an Airplane. NACA ACR No. L4E30, 1944.

3. Batson, A.S., Preston, J.H., and Warsap, J.H.: Effect on Hinge Moment of Modifying the Section of a Control and in Each Case of Fitting Trailing Edge Strips and a Shrouded Balance. Rep. 5062, S. & C. 1224, British A.R.C., May 1944.

4. Halliday, A.S., Sweeting, N.E., and Skelton, W.S.: Investigation of the Effect of Change of Section on Rudder Hinge Moments. Rep. 5266, S. & C. 1249, British A.R.C., Aug. 1944.

5. Hall, Charles F., and Mannes, Robert L.: Longitudinal Characteristics and Aileron Effectiveness of a Mid-wing Airplane from High-Speed Wind-Tunnel Tests. NACA CMR, Sept. 1944.

6. Purser, Paul E., and Gillis, Clarence L.: Preliminary Correlation of the Effects of Beveled Trailing Edges on the Hinge-Moment Characteristics of Control Surfaces. NACA CB No. 3E14, 1943.

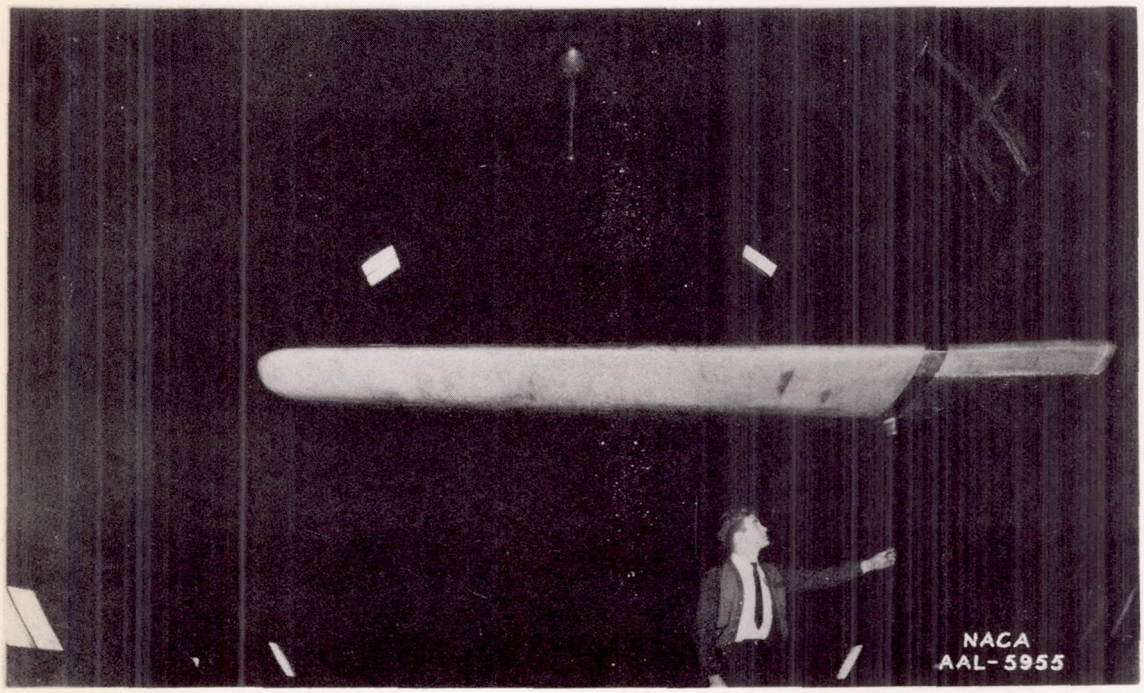

Figure 1.- A full-scale semispan horizontal tail for the bomber airplane in the 16-foot wind tunnel.

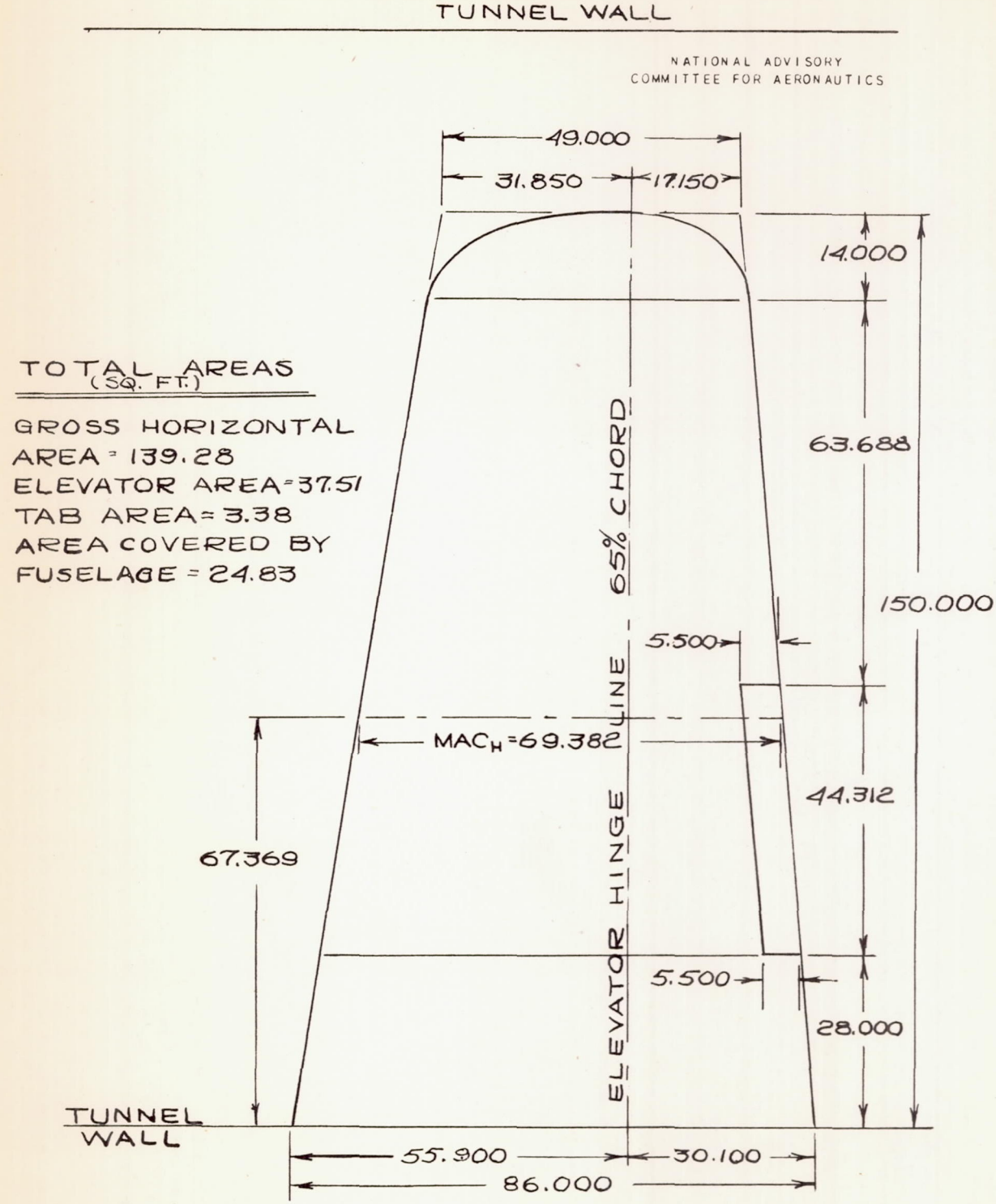

FIGURE 2.- PLAN VIEW OF A SEMISPAN HORIZONTAL TAIL FOR THE BOMBER AIRPLANE.

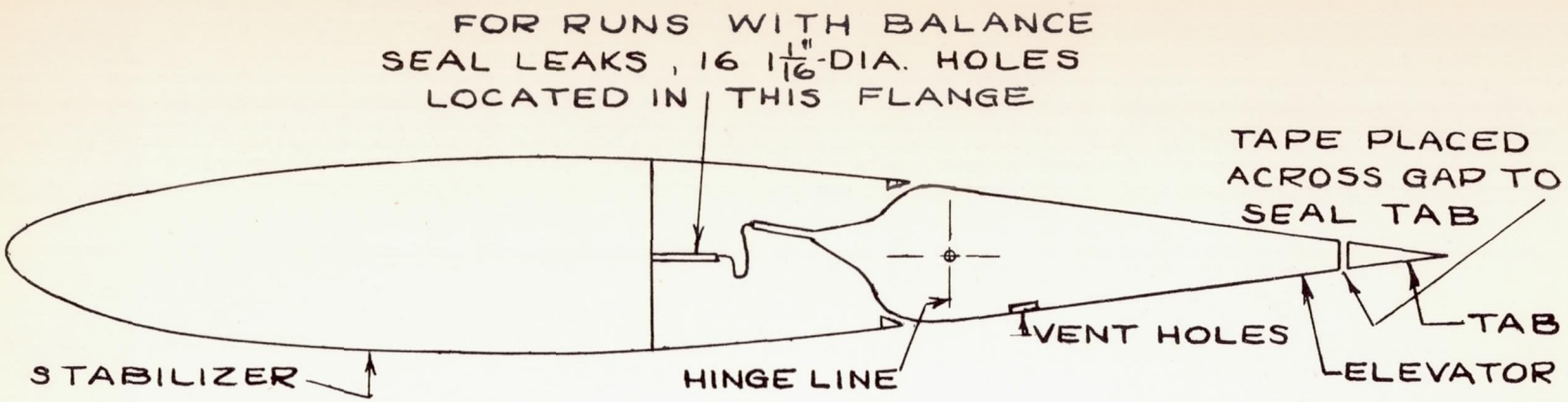

AIRFOIL CONTOUR - DOUGLAS F_1
PERCENT THICKNESS - 13.45 CONSTANT
APPROXIMATE ELEVATOR BALANCE SPAN - 105 IN.
BALANCE CHORD RATIO 45%
DIHEDRAL - 0°
AIRFOIL HAS NEGATIVE CAMBER AS INSTALLED

NATIONAL ADVISORY
COMMITTEE FOR AERONAUTICS

FIGURE 3. - TYPICAL CROSS SECTION OF A SEMISPAN HORIZONTAL TAIL OF THE BOMBER AIRPLANE.

MR NO. A4L18

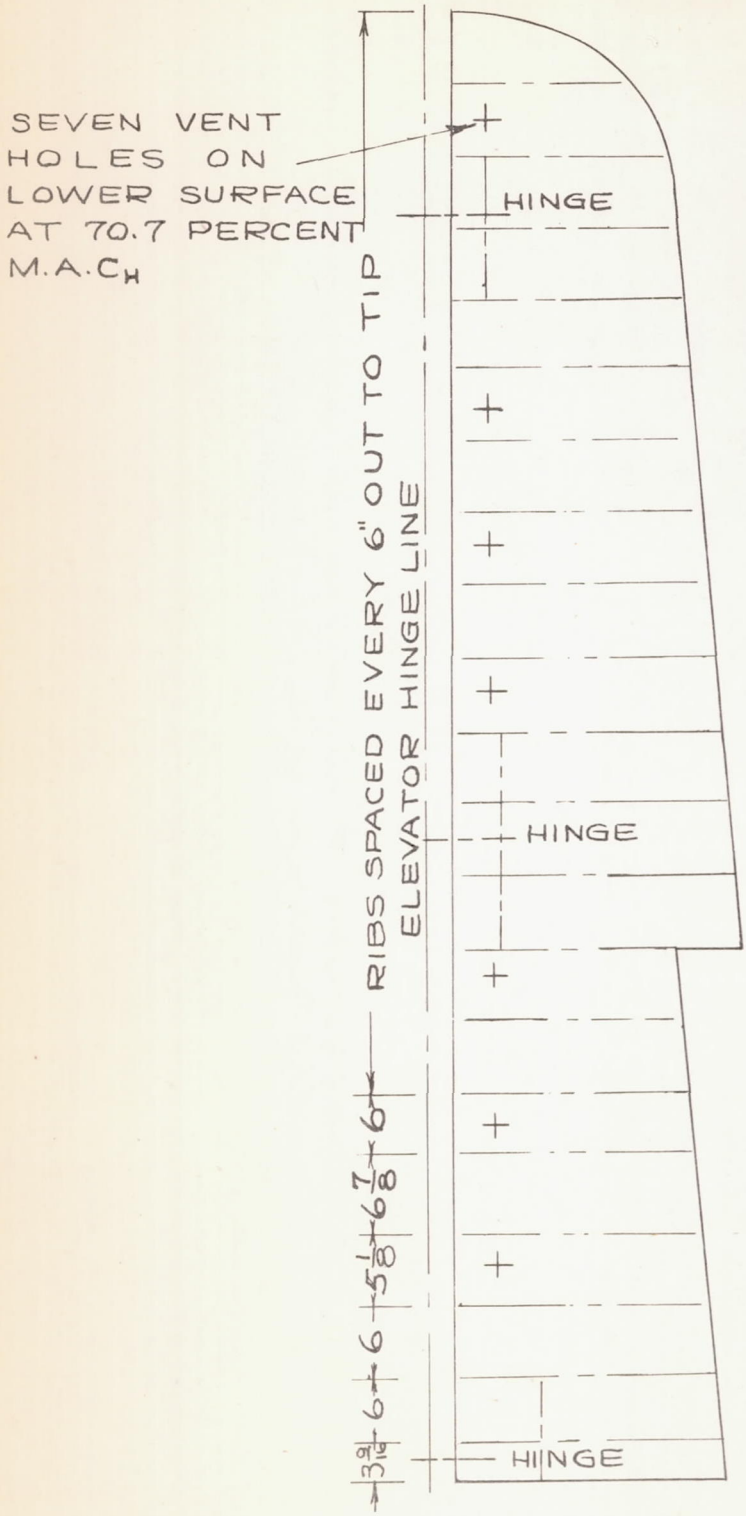

SPECIFICATIONS

1. FABRIC - COTTON AIRPLANE CLOTH AN-CCC-O-399.
2. DOPED WITH 4 COATS CLEAR NITRATE DOPE - AN-TT-D-154. APPLIED BY HAND, 2 COATS ALUMINIZED DOPE - AN-TT-D-551. APPLIED BY SPRAY, USING PROCEDURE 98-24-100. DRIED IN TEMPERATURE CONTROLLED ROOM.
3. SAME PROCESS FOLLOWED AS WITH PRODUCTION AIRPLANE, IN DOPING STITCHING, ETC.

NATIONAL ADVISORY COMMITTEE FOR AERONAUTICS

FIGURE 4. - THE RIB SPACING OF THE FABRIC-COVERED ELEVATOR FOR THE SEMISPAN HORIZONTAL TAIL OF THE BOMBER AIRPLANE.

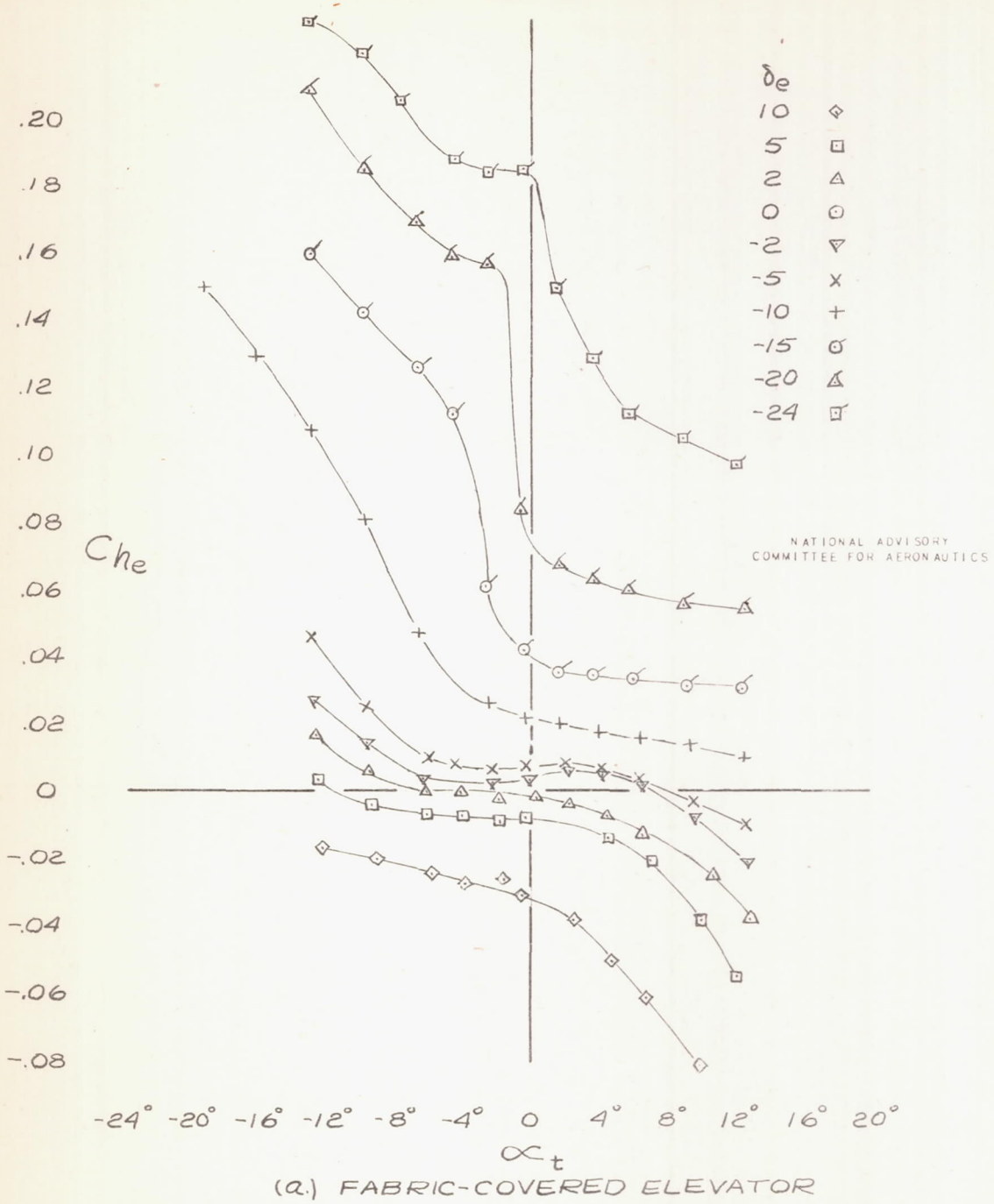

(a.) FABRIC-COVERED ELEVATOR

FIGURE 5. - VARIATION OF HINGE-MOMENT COEFFICIENT WITH TAIL ANGLE OF ATTACK. M, 0.133 ; δ_t, 0°.

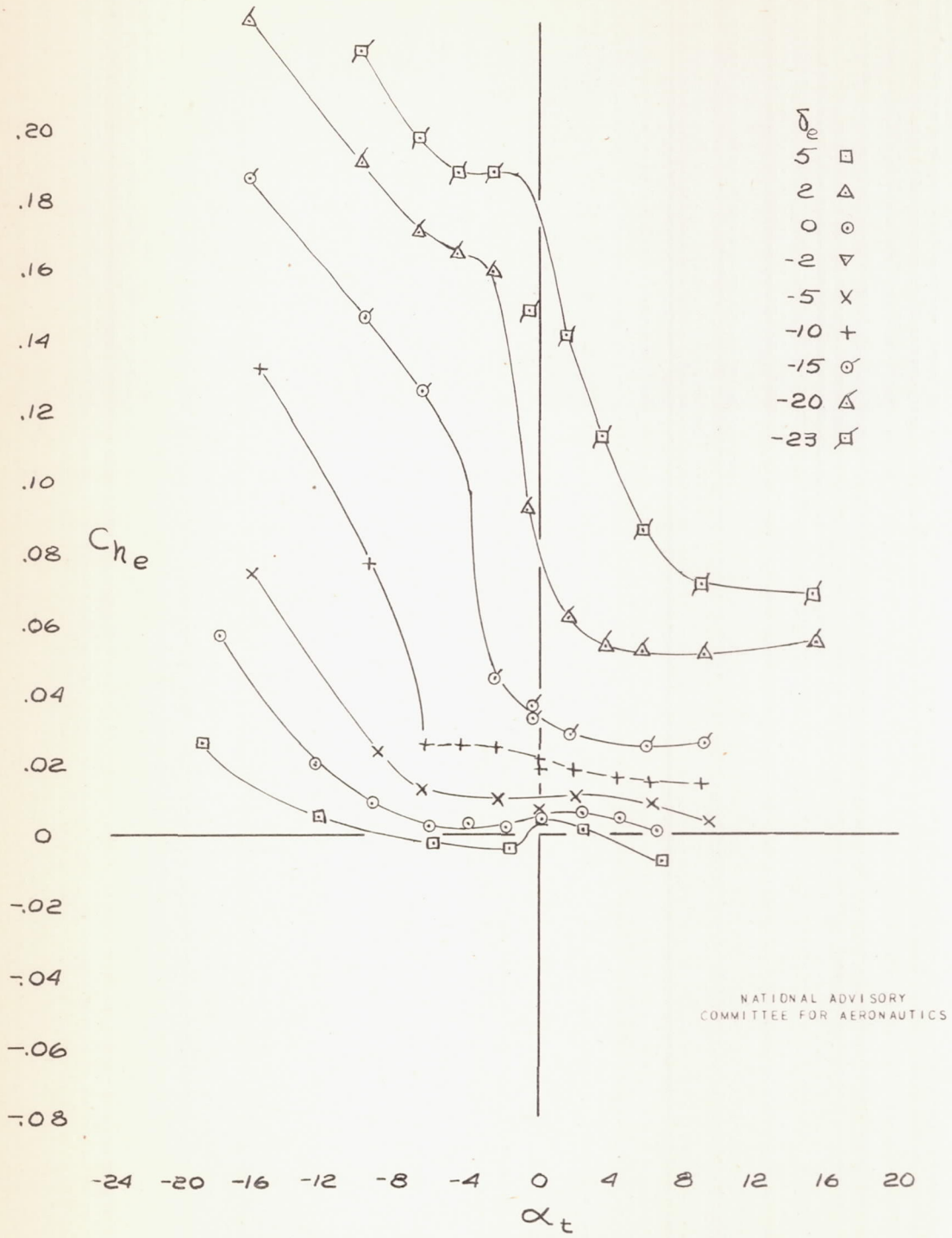

(b) METAL-COVERED ELEVATOR

FIGURE 5. - CONCLUDED.

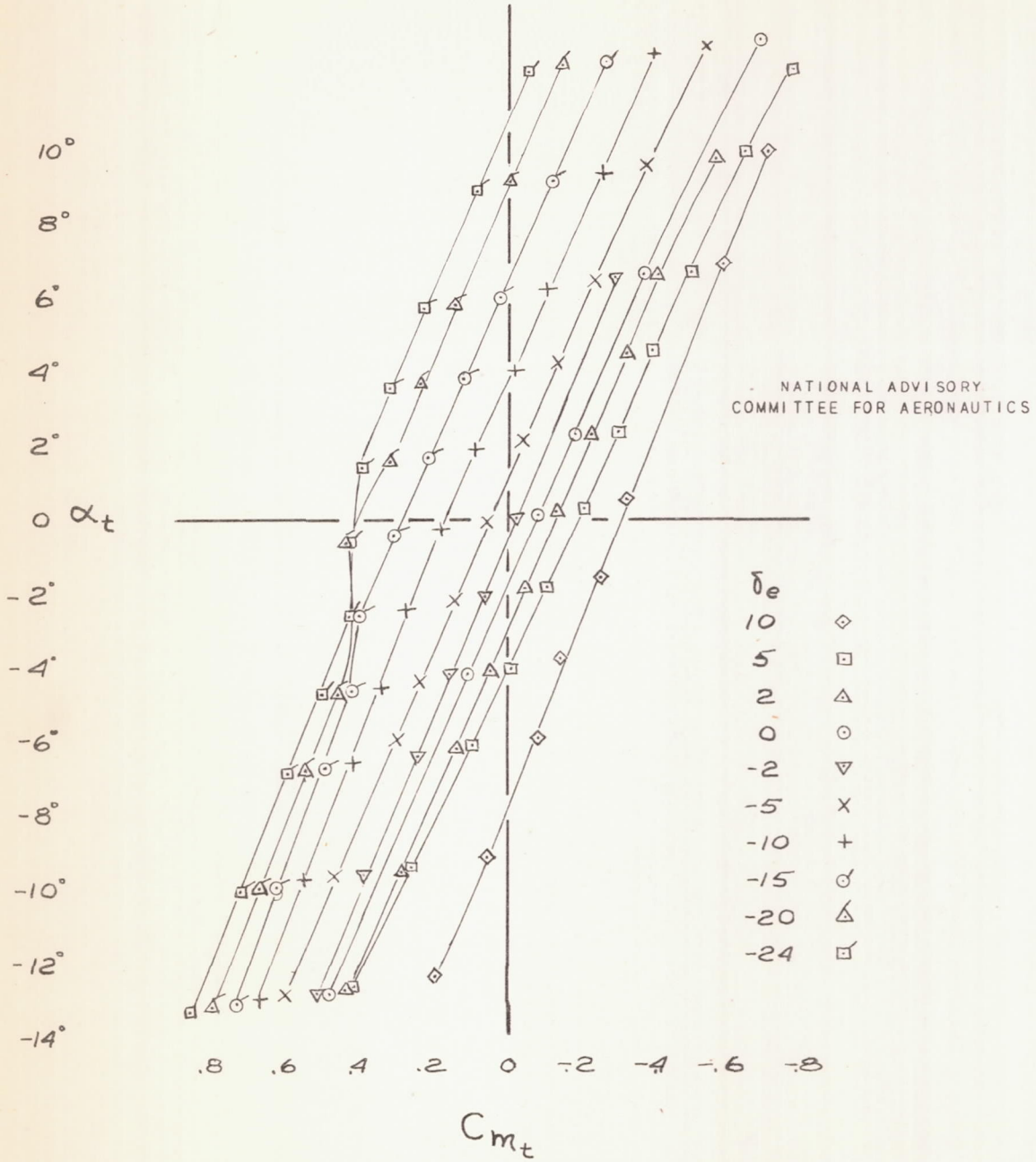

(a) FABRIC-COVERED ELEVATOR.

FIGURE 6.- VARIATION OF PITCHING-MOMENT COEFFICIENT DUE TO THE TAIL WITH TAIL ANGLE OF ATTACK. M, 0.133; δ_t, 0°.

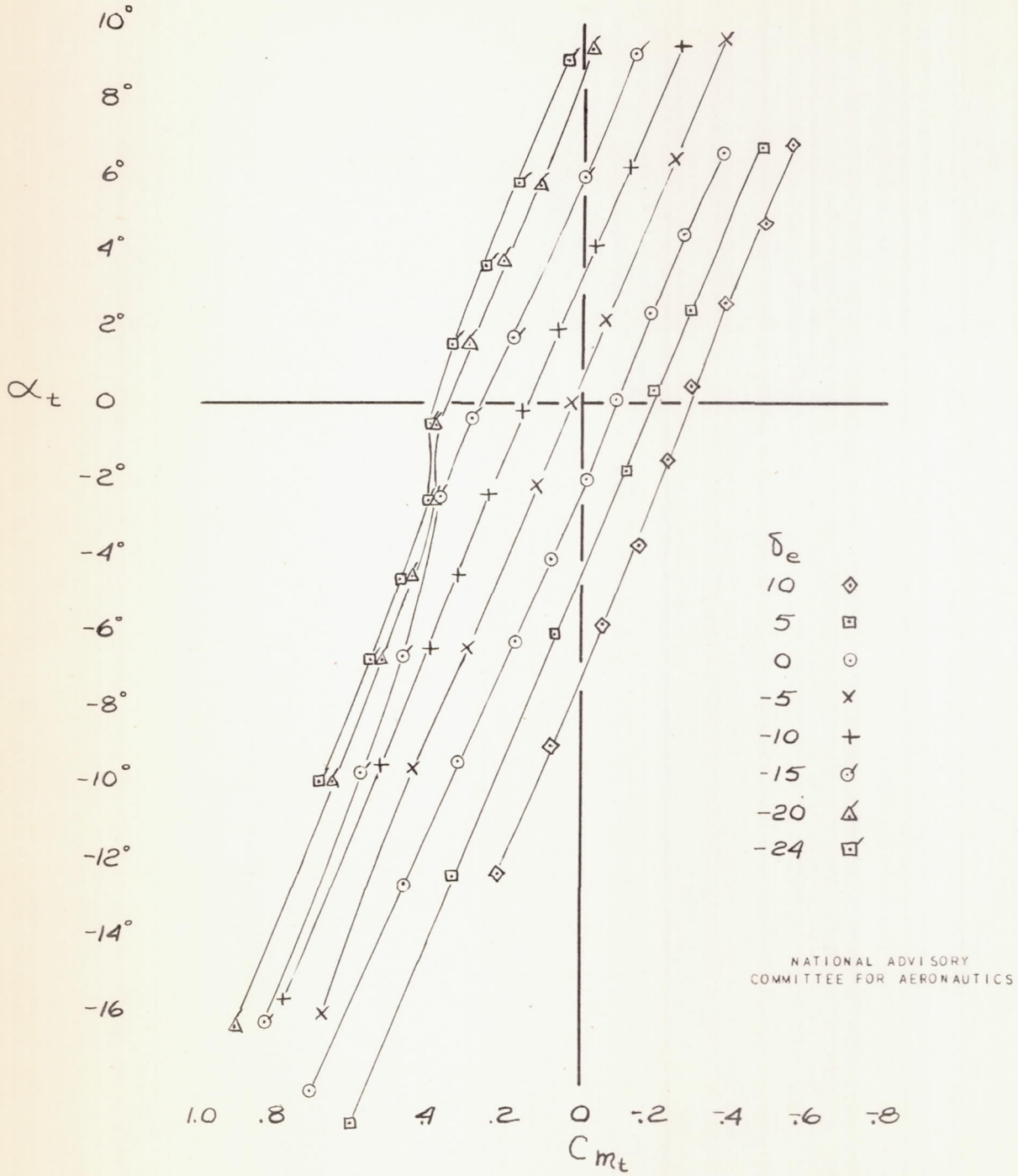

(b) METAL-COVERED ELEVATOR

FIGURE 6.- CONCLUDED.

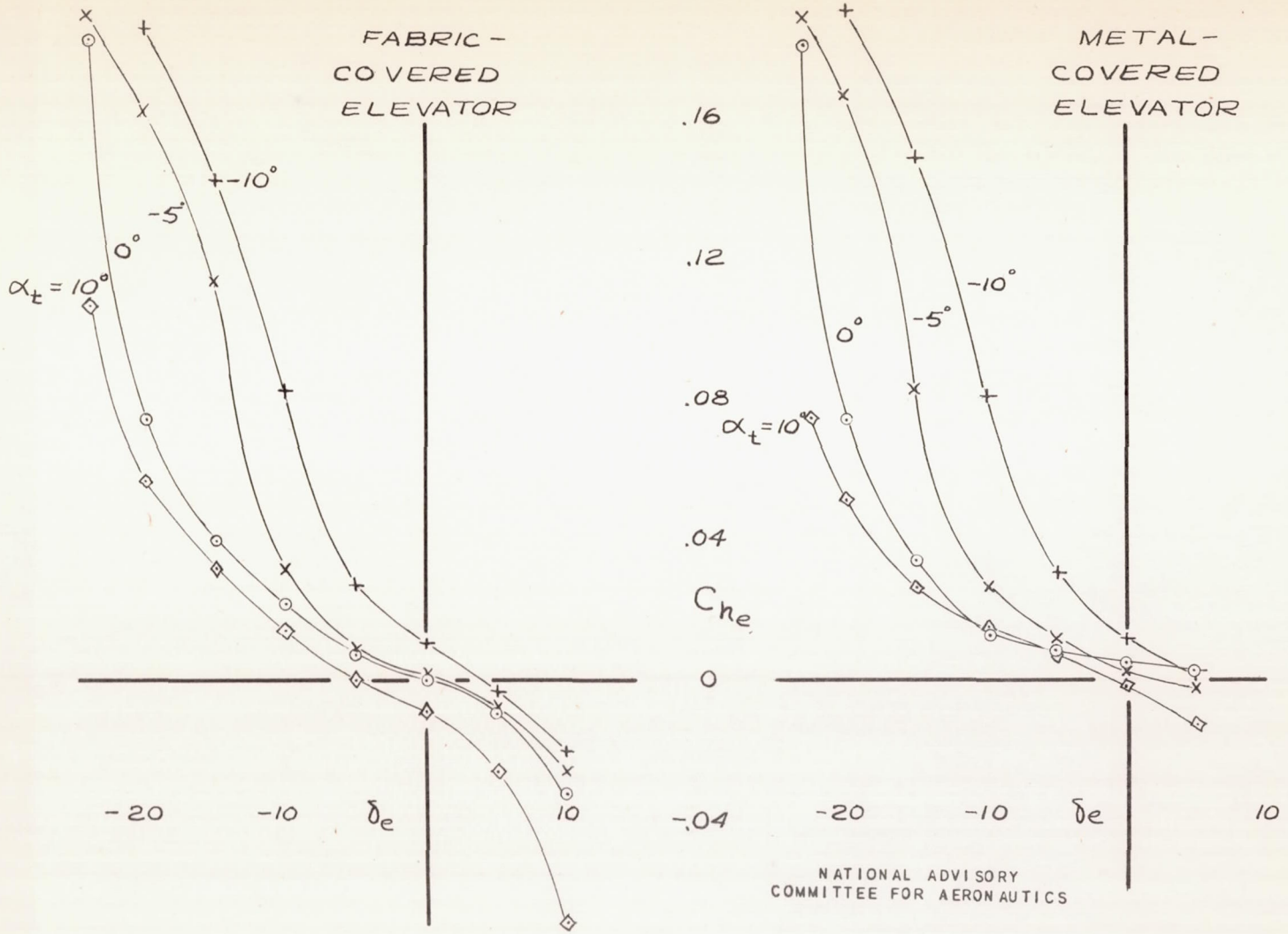

FIGURE 7.- VARIATION OF ELEVATOR HINGE-MOMENT COEFFICIENT WITH ELEVATOR ANGLE. M_1 0.133; δ_t 0°;

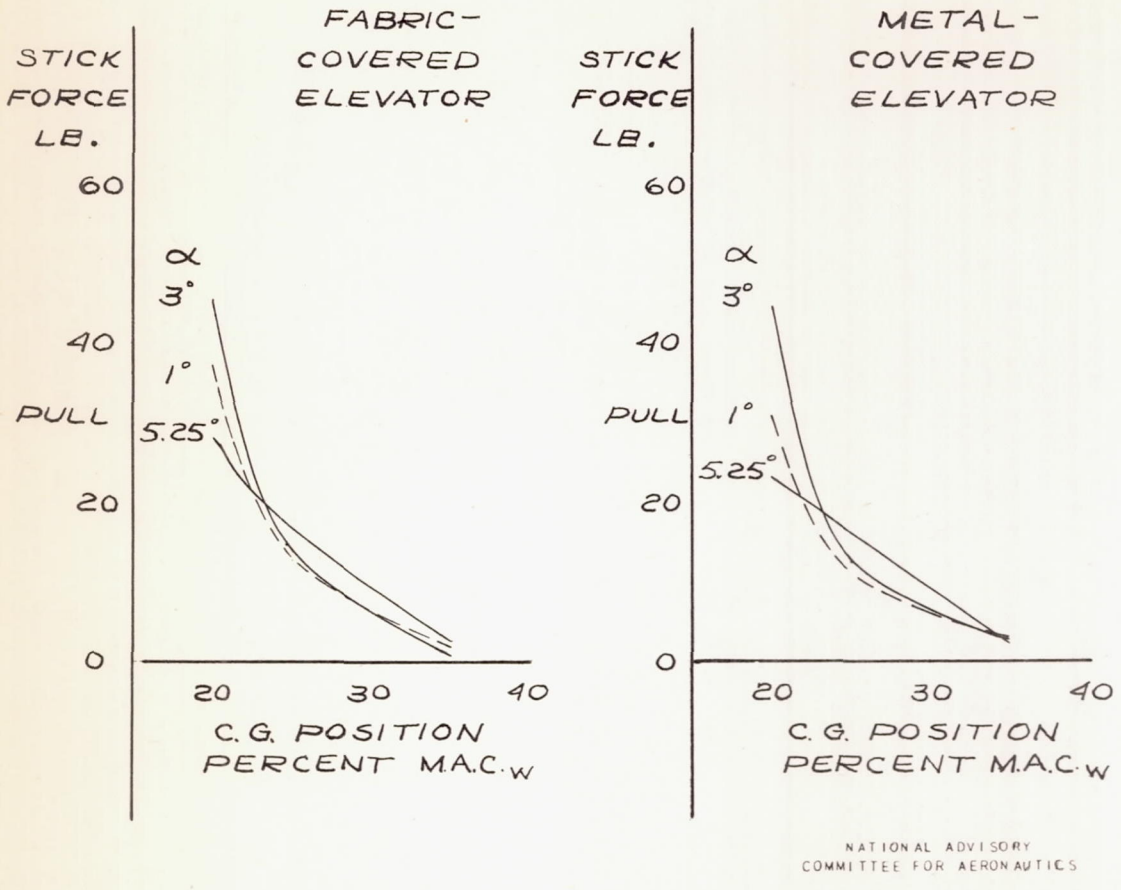

FIGURE 8.- VARIATION OF ELEVATOR STICK FORCE WITH C.G. POSITION, LANDING WITH FLAPS DOWN. M, 0.133; δ_t, 0°.

A83

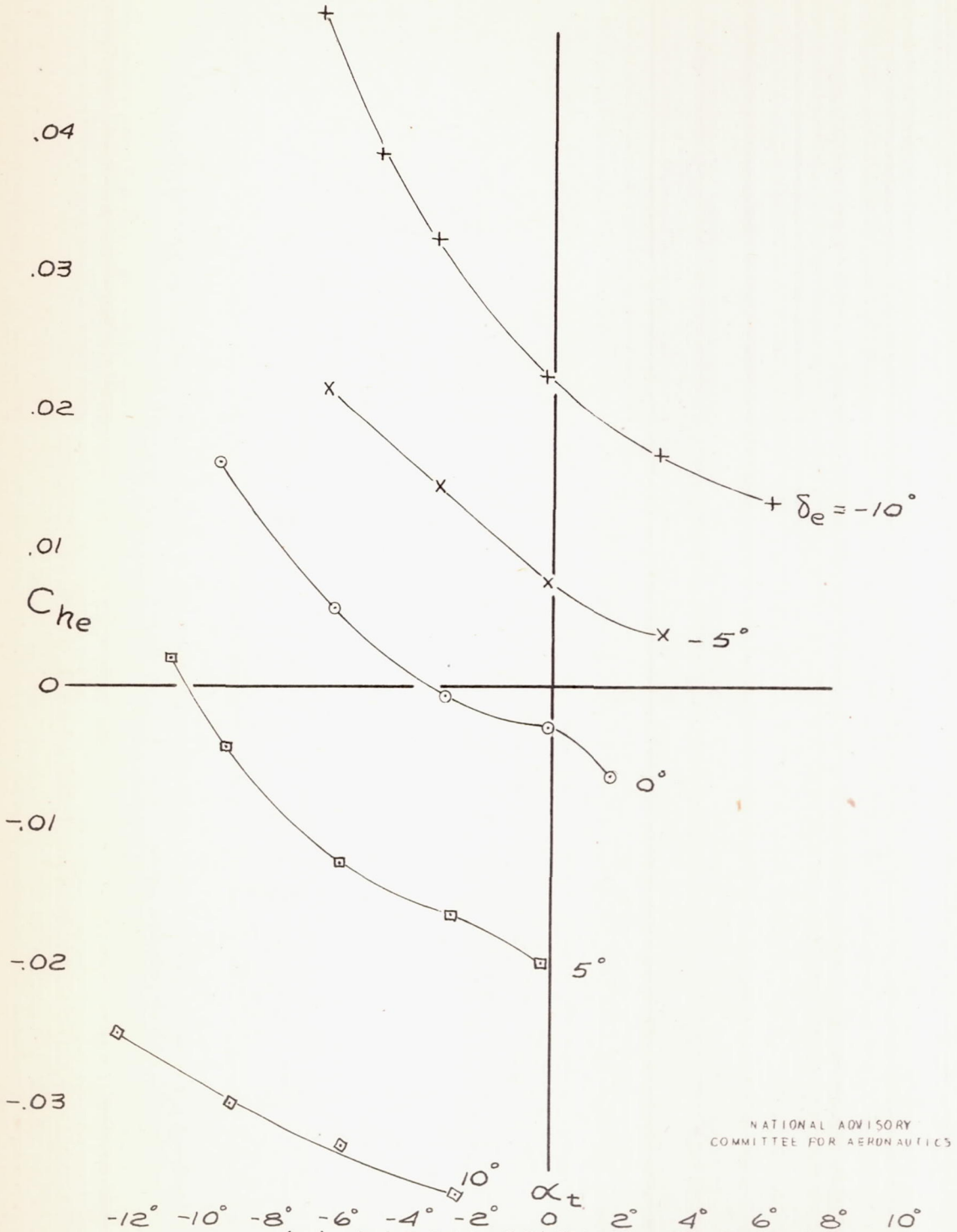

(a) FABRIC-COVERED ELEVATOR

FIGURE 9.- VARIATION OF HINGE-MOMENT COEFFICIENT WITH TAIL ANGLE OF ATTACK. M, 0.33; δ_t, 0°

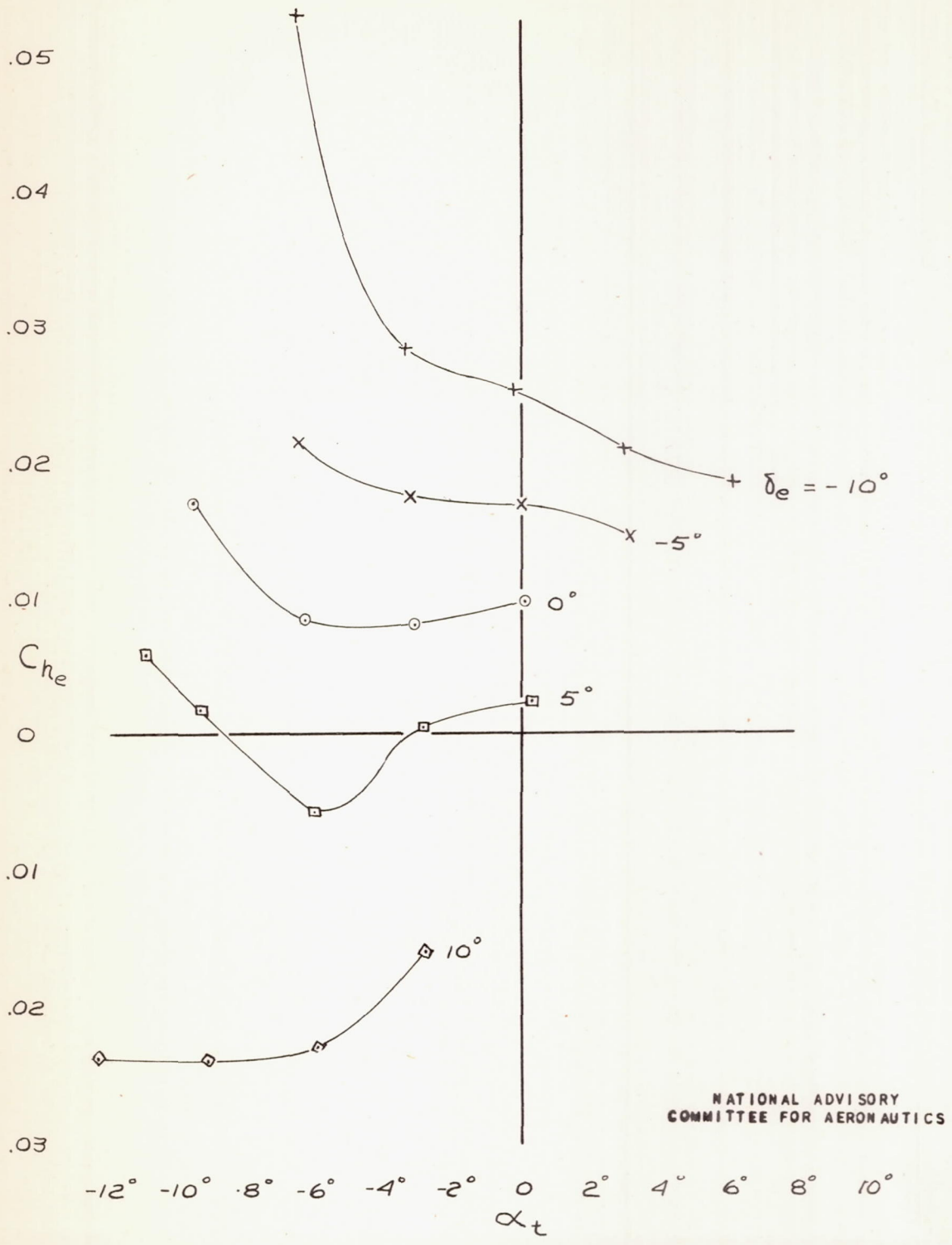

(b) METAL-COVERED ELEVATOR

FIGURE 9.- CONCLUDED.

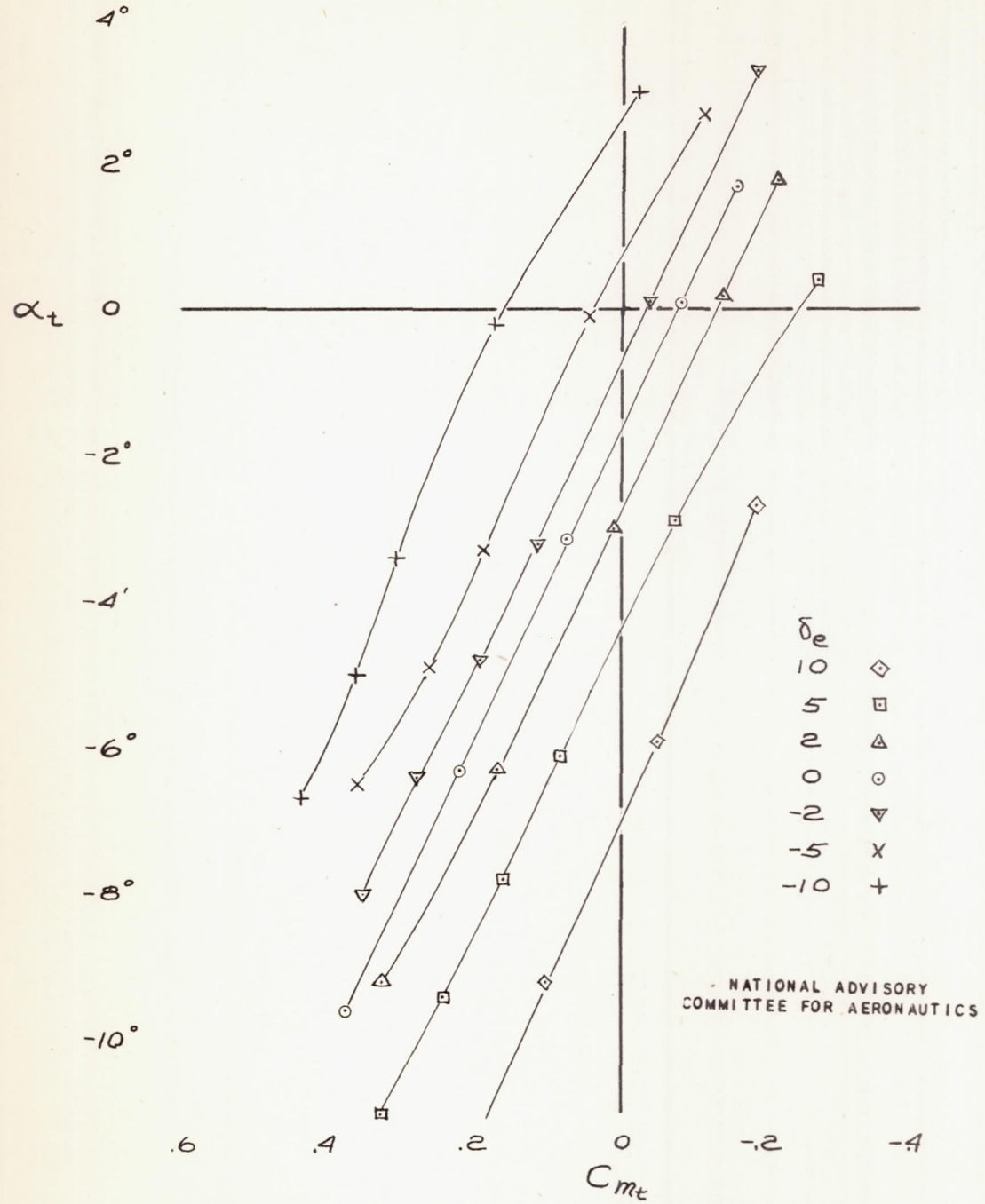

(a) FABRIC - COVERED ELEVATOR.

FIGURE 10. - VARIATION OF PITCHING-MOMENT COEFFICIENT DUE TO THE TAIL WITH TAIL ANGLE OF ATTACK. M, 0.33; δ_t, 0°.

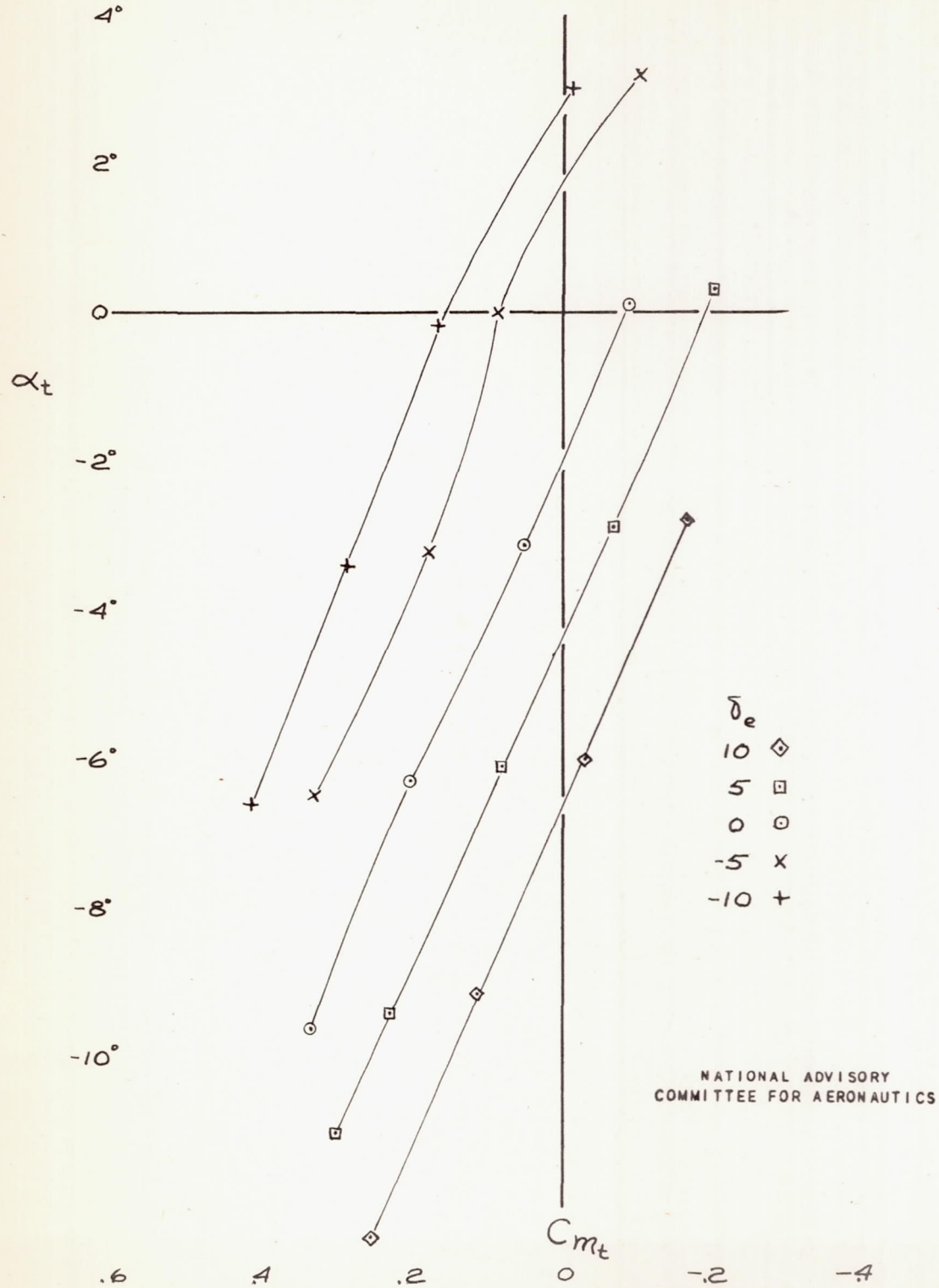

(b) METAL-COVERED ELEVATOR

FIGURE 10.- CONCL

NATIONAL ADVISORY
COMMITTEE FOR AERONAUTICS

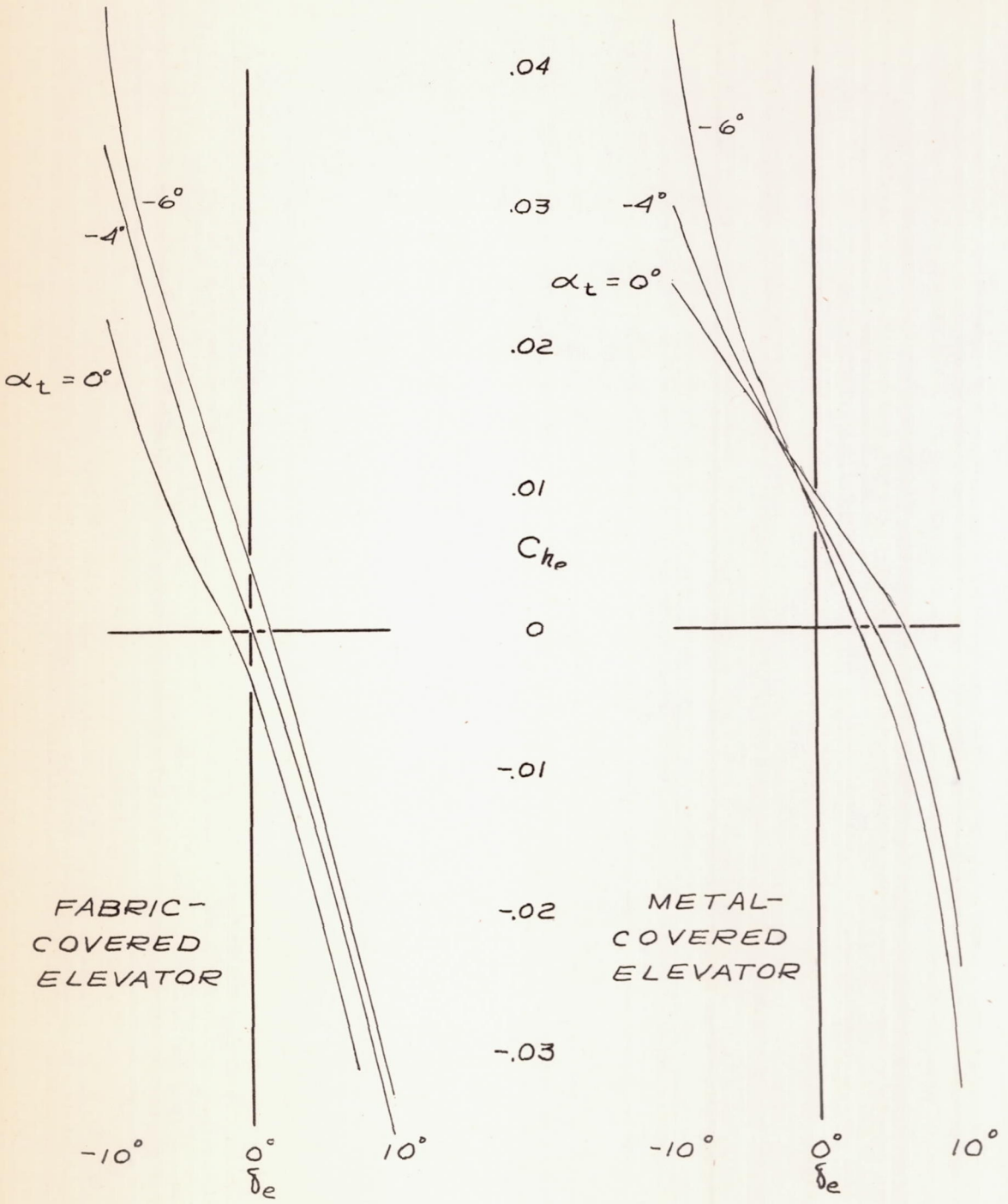

FIGURE 11.- VARIATION OF ELEVATOR HINGE-MOMENT COEFFICIENT WITH ELEVATOR ANGLE, M, 0.33; δ_t, 0°.

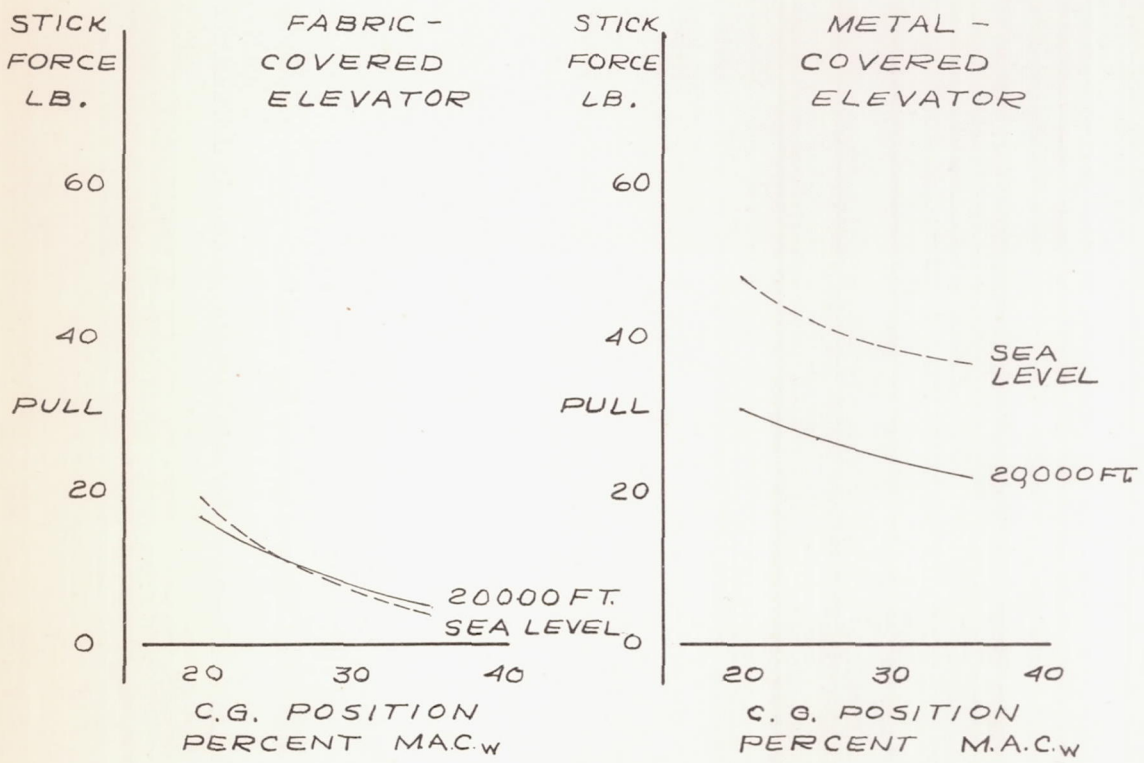

NATIONAL ADVISORY
COMMITTEE FOR AERONAUTICS

FIGURE 12.- VARIATION OF ELEVATOR STICK FORCE WITH C.G. POSITION, M, 0.33; δ_t, 0°; WEIGHT 25000 LB.; LEVEL FLIGHT;

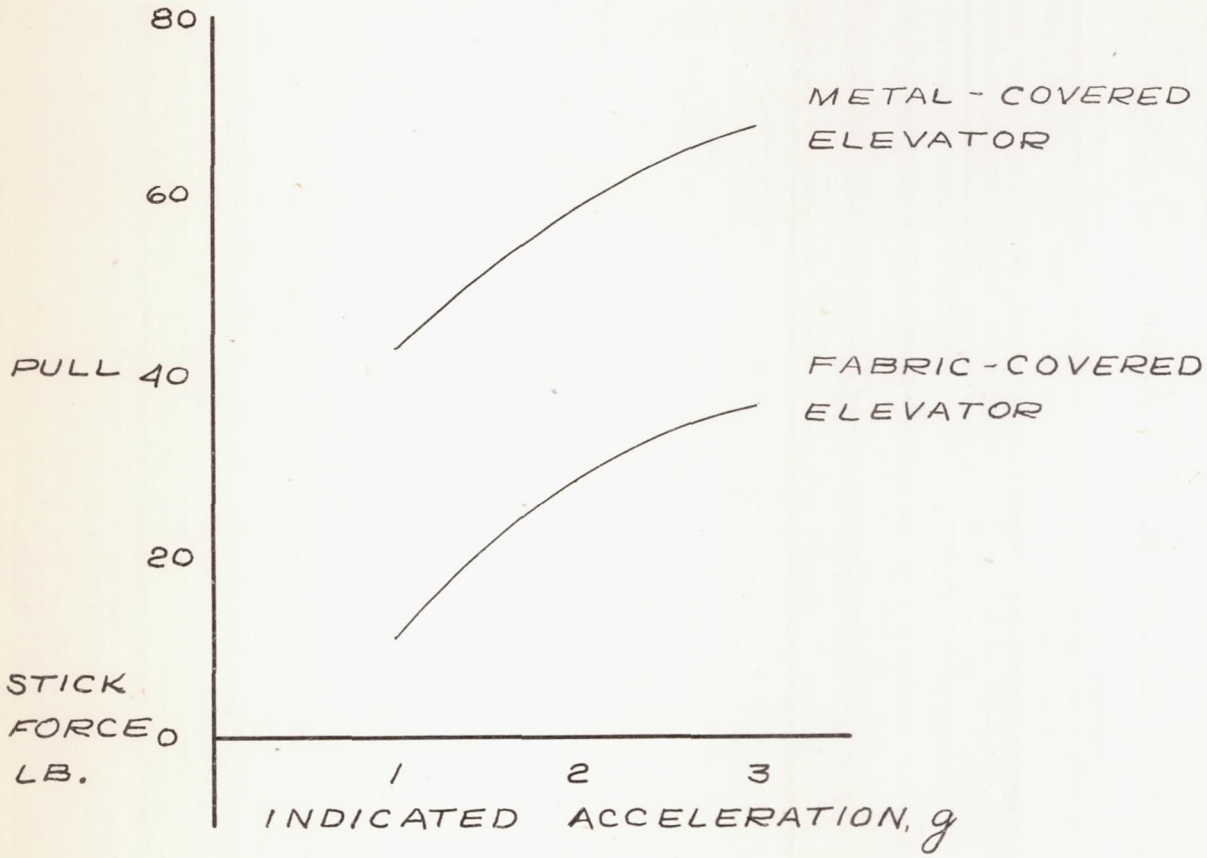

NATIONAL ADVISORY
COMMITTEE FOR AERONAUTICS

FIGURE 13.— VARIATION OF ELEVATOR STICK FORCE WITH ACCELERATION AT SEA LEVEL; C.G. AT 25% M.A.C.$_W$; WEIGHT, 25000 LB.

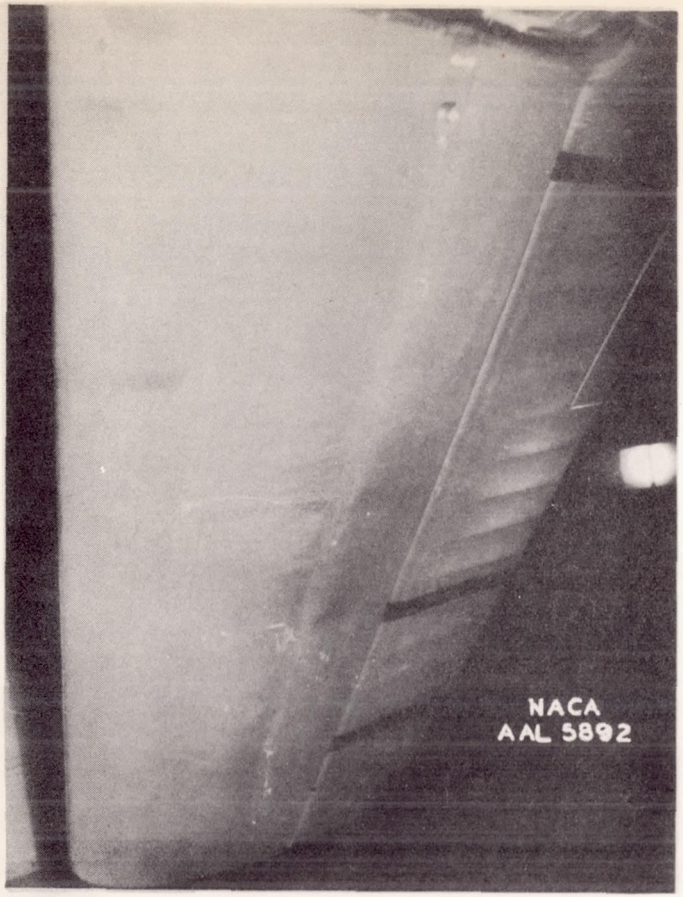

(a) Upper surface.

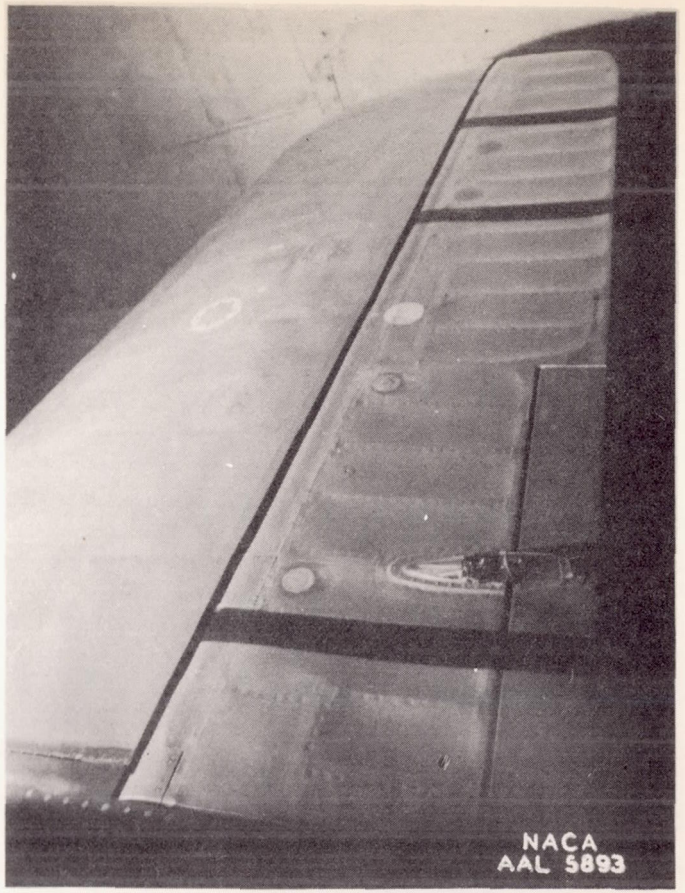

(b) Lower surface.

Figure 14.- The bomber stabilizer with the fabric-covered elevator. M, 0.72; α_t, -3°; δ_e, 0°.

(a) Upper surface.

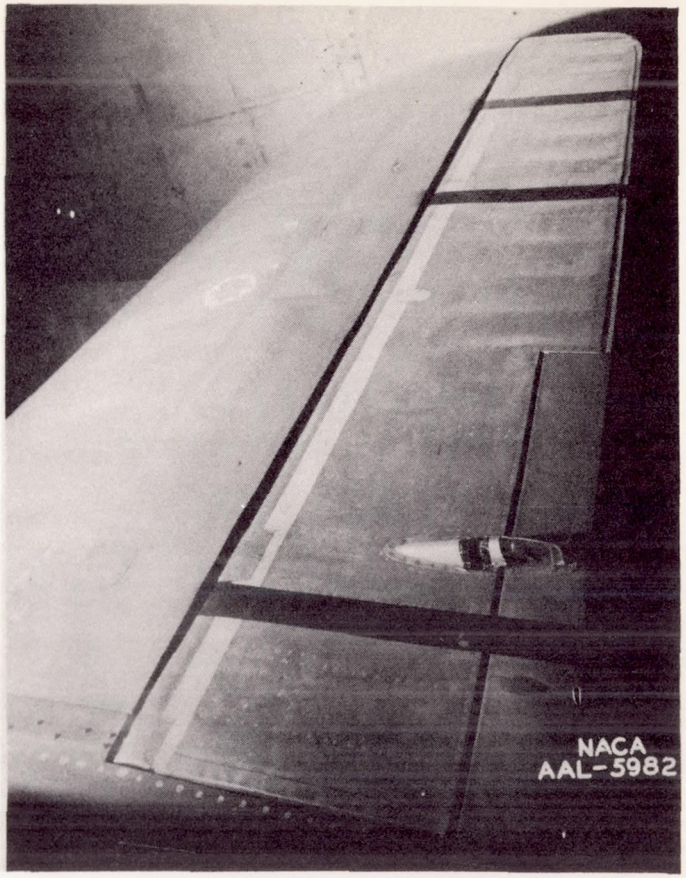

(b) Lower surface

Figure 15.- The bomber stabilizer with the metal-covered elevator. M, 0.72; α_t, -3°; δ_e, 0°.

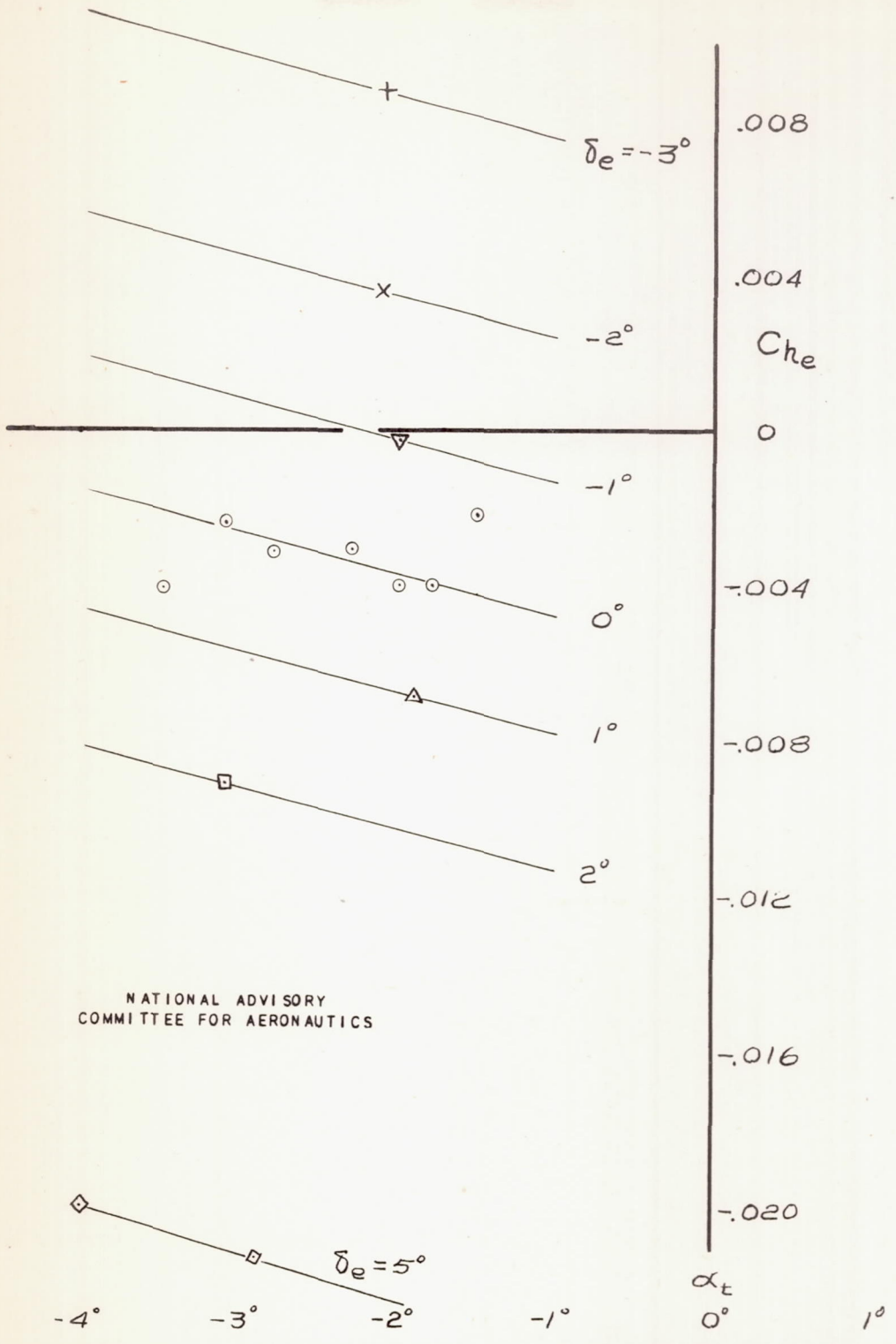

(a) FABRIC-COVERED ELEVATOR

FIGURE 16.- VARIATION OF HINGE-MOMENT COEFFICIENT WITH TAIL ANGLE OF ATTACK. M, 0.72 ; δ_t, 0°.

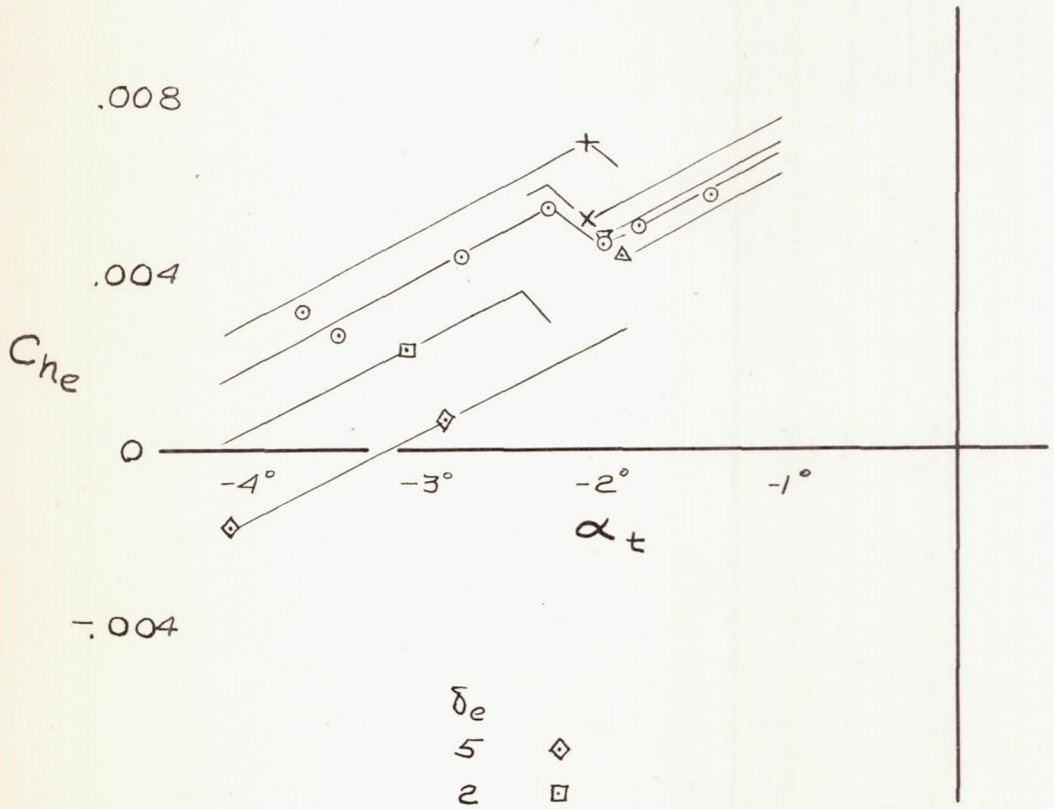

(b) METAL-COVERED ELEVATOR.

FIGURE 16.- CONCLUDED.

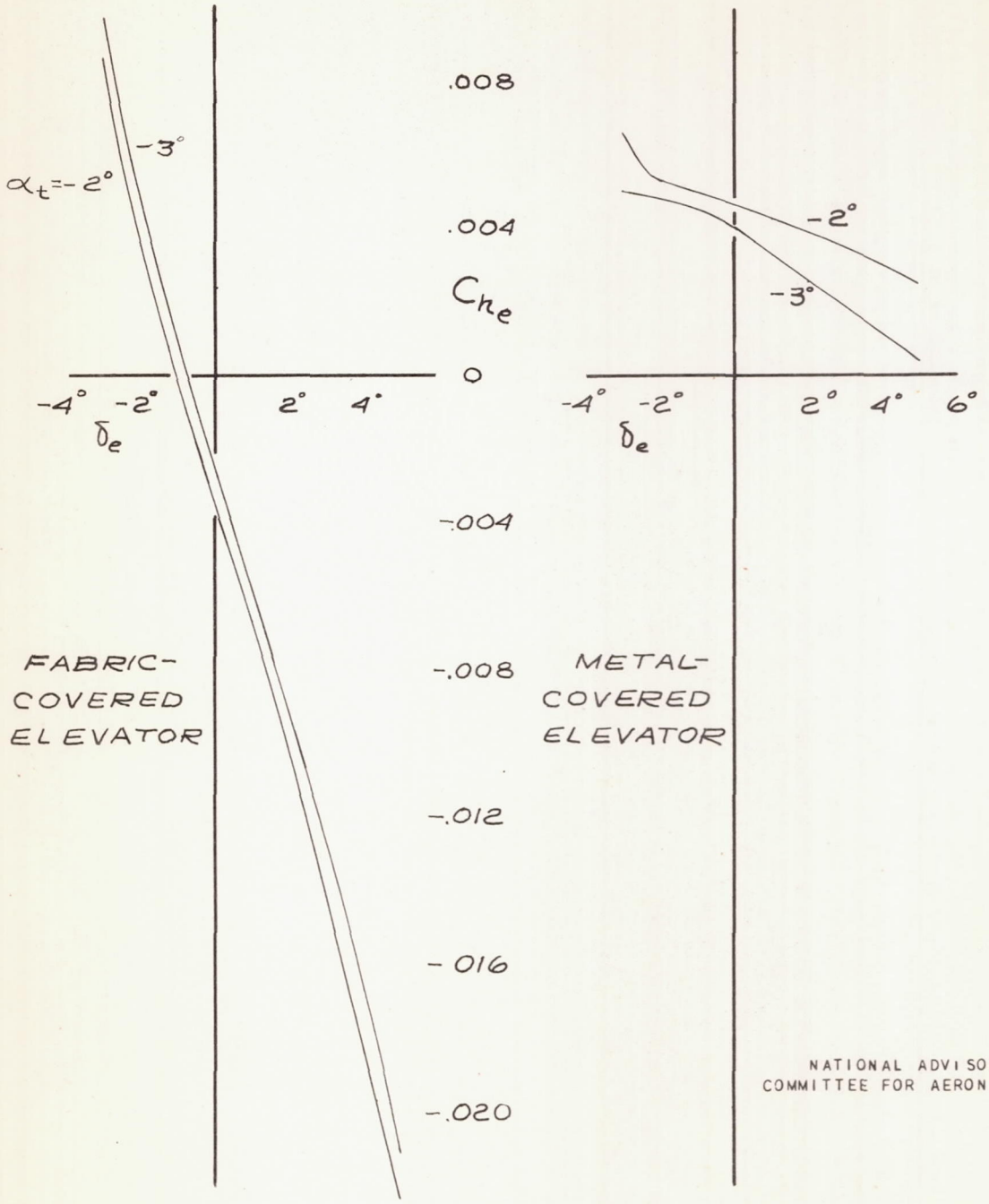

FIGURE 17.- VARIATION OF ELEVATOR HINGE-MOMENT COEFFICIENT WITH ELEVATOR ANGLE. M, 0.72; δ_t, 0°.

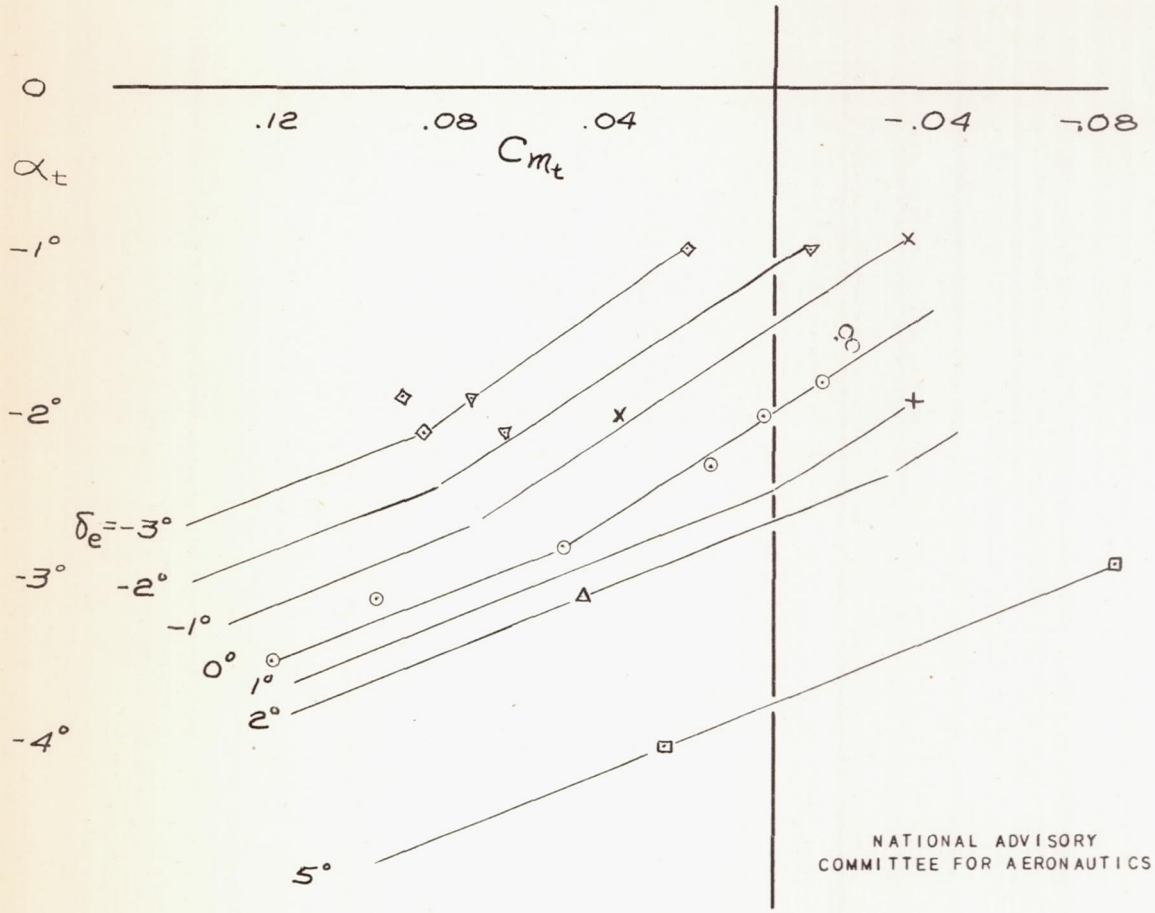

(a) FABRIC-COVERED ELEVATOR

FIGURE 18.- VARIATION OF PITCHING-MOMENT COEFFICIENT DUE TO THE TAIL WITH TAIL ANGLE OF ATTACK. M, 0.72; δ_t, 0°.

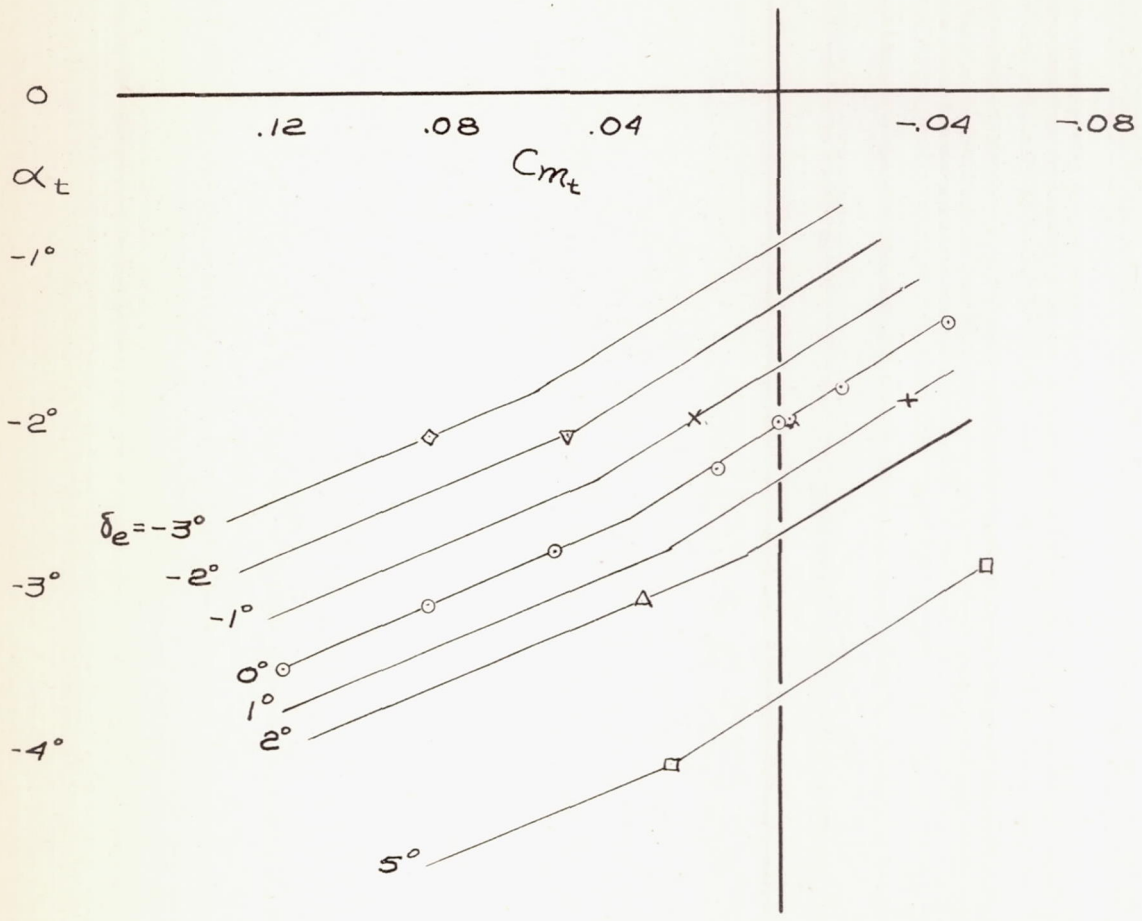

NATIONAL ADVISORY
COMMITTEE FOR AERONAUTICS

(d) METAL-COVERED ELEVATOR.

FIGURE 18.- CONCLUDED.

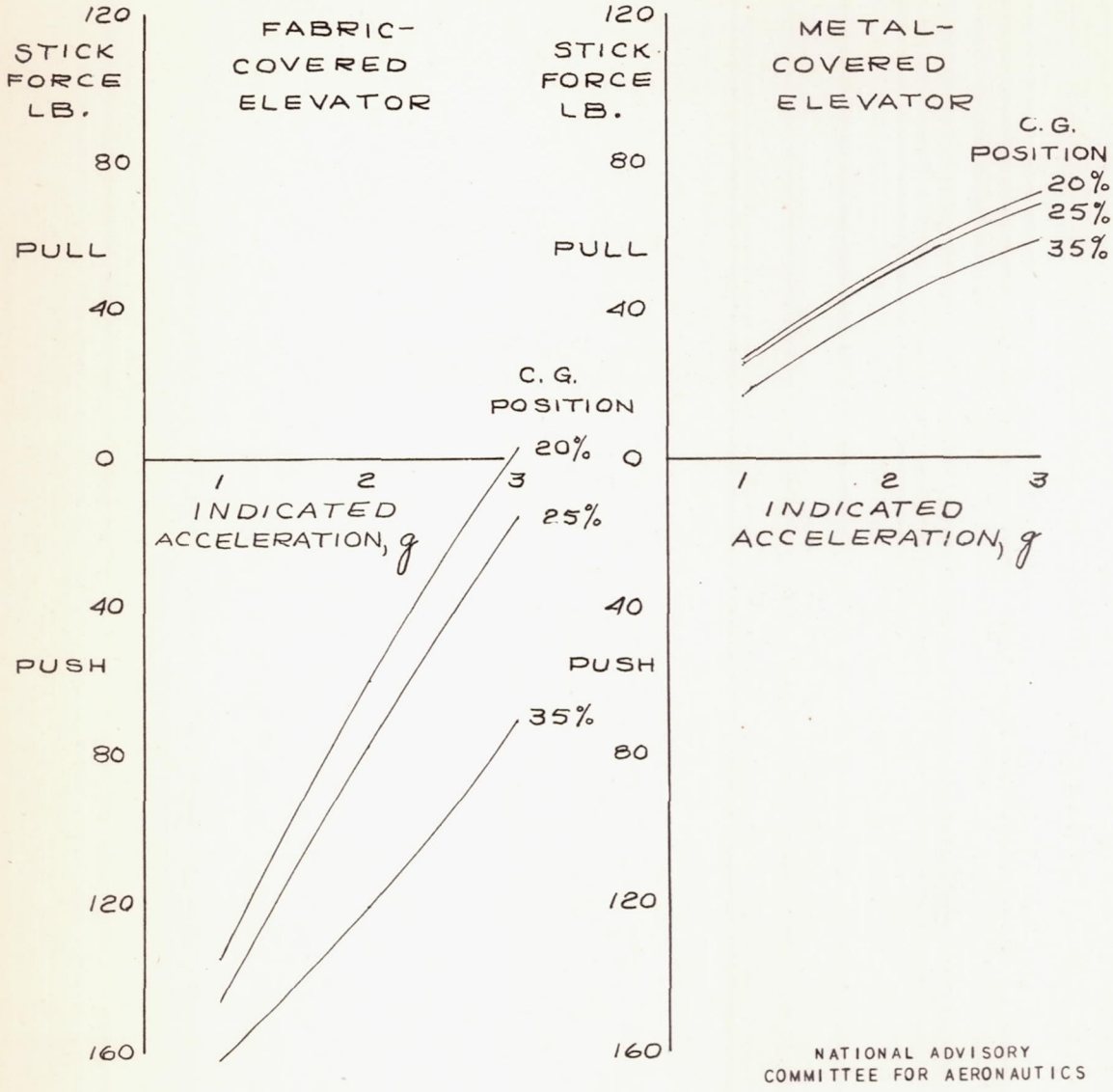

(a) SEA LEVEL

FIGURE 19.- VARIATION OF ELEVATOR STICK FORCE WITH INDICATED ACCELERATION AT M_1 0.72; δ_{t_1} 0°.

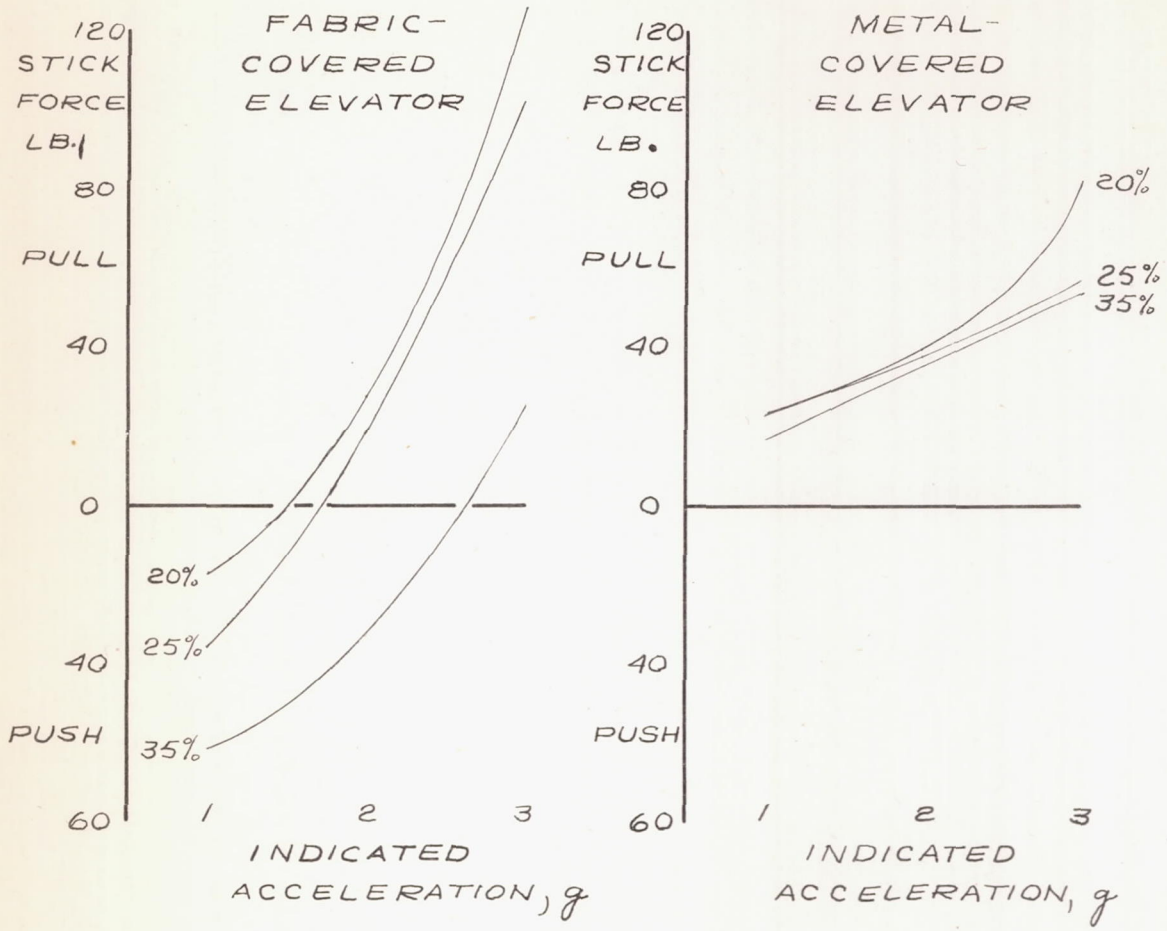

NATIONAL ADVISORY
COMMITTEE FOR AERONAUTICS

(b) 20,000 FT.

FIGURE 19.-CONCLUDED.

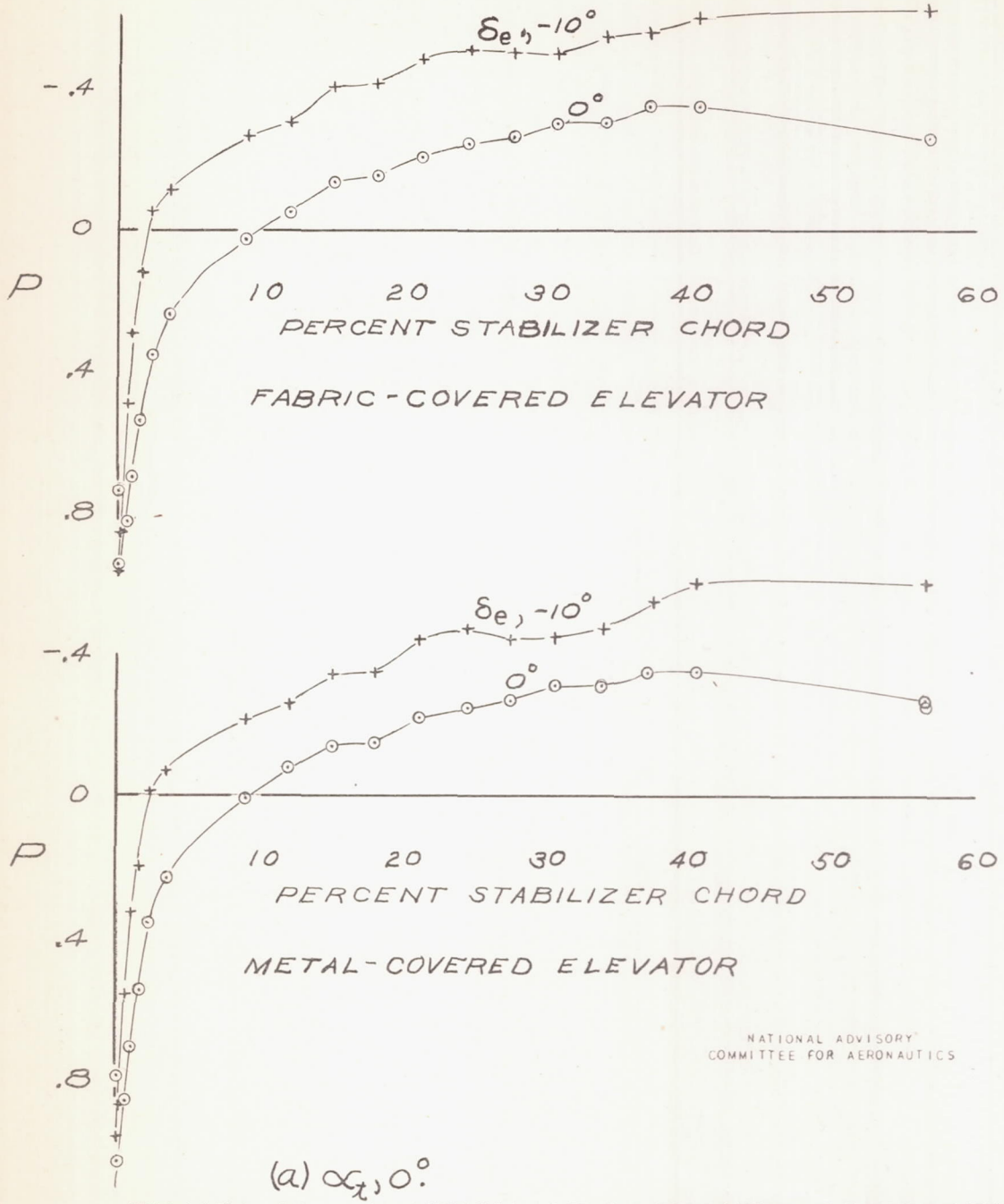

(a) α_t, 0°.

FIGURE 20.-VARIATION OF PRESSURE COEFFICIENT WITH CHORDWISE STATION ON THE LOWER SURFACE. M, 0.33; δ_t, 0°; STATION 92.

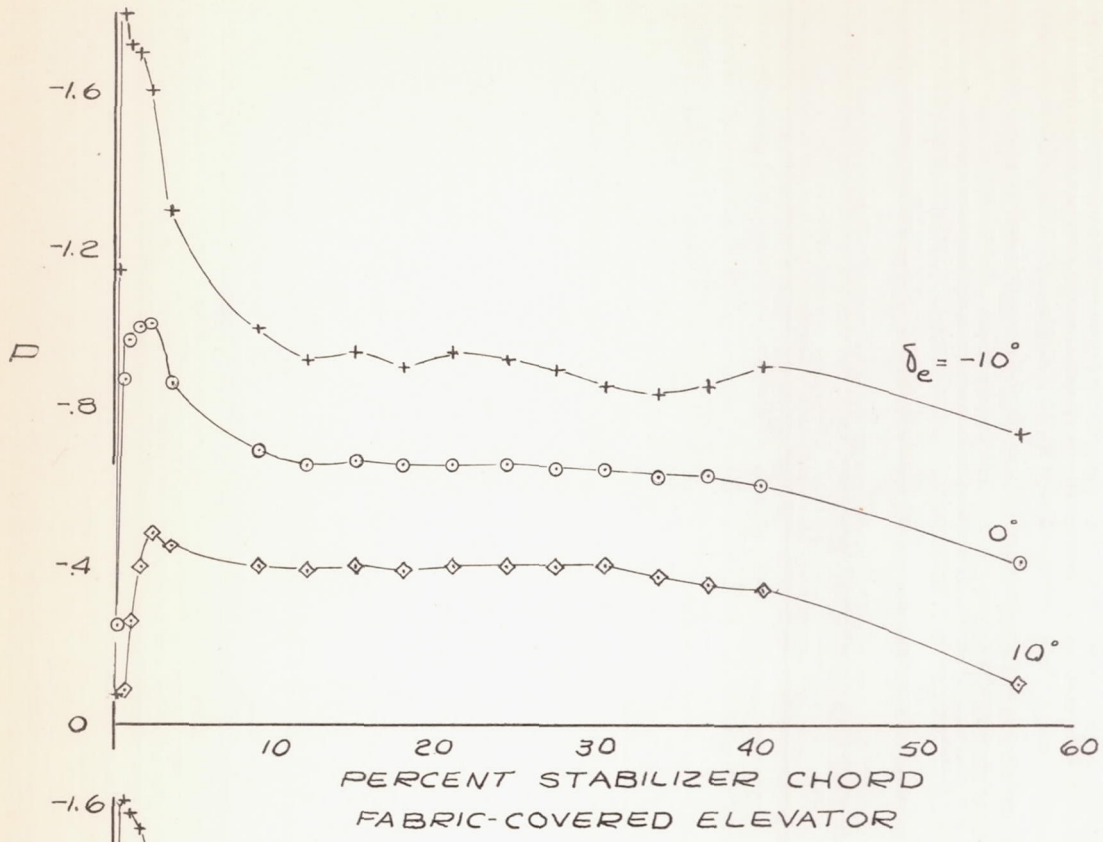

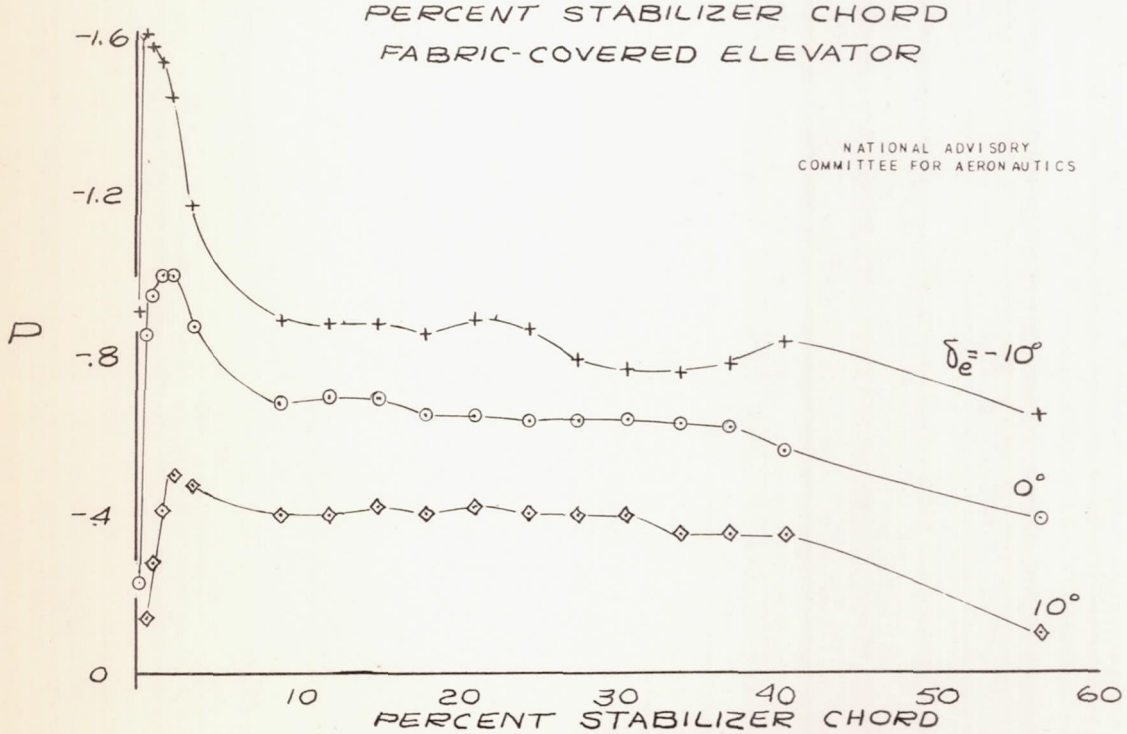

NATIONAL ADVISORY
COMMITTEE FOR AERONAUTICS

(b) $\alpha_t - 6°$

FIGURE 20.- CONCLUDED.

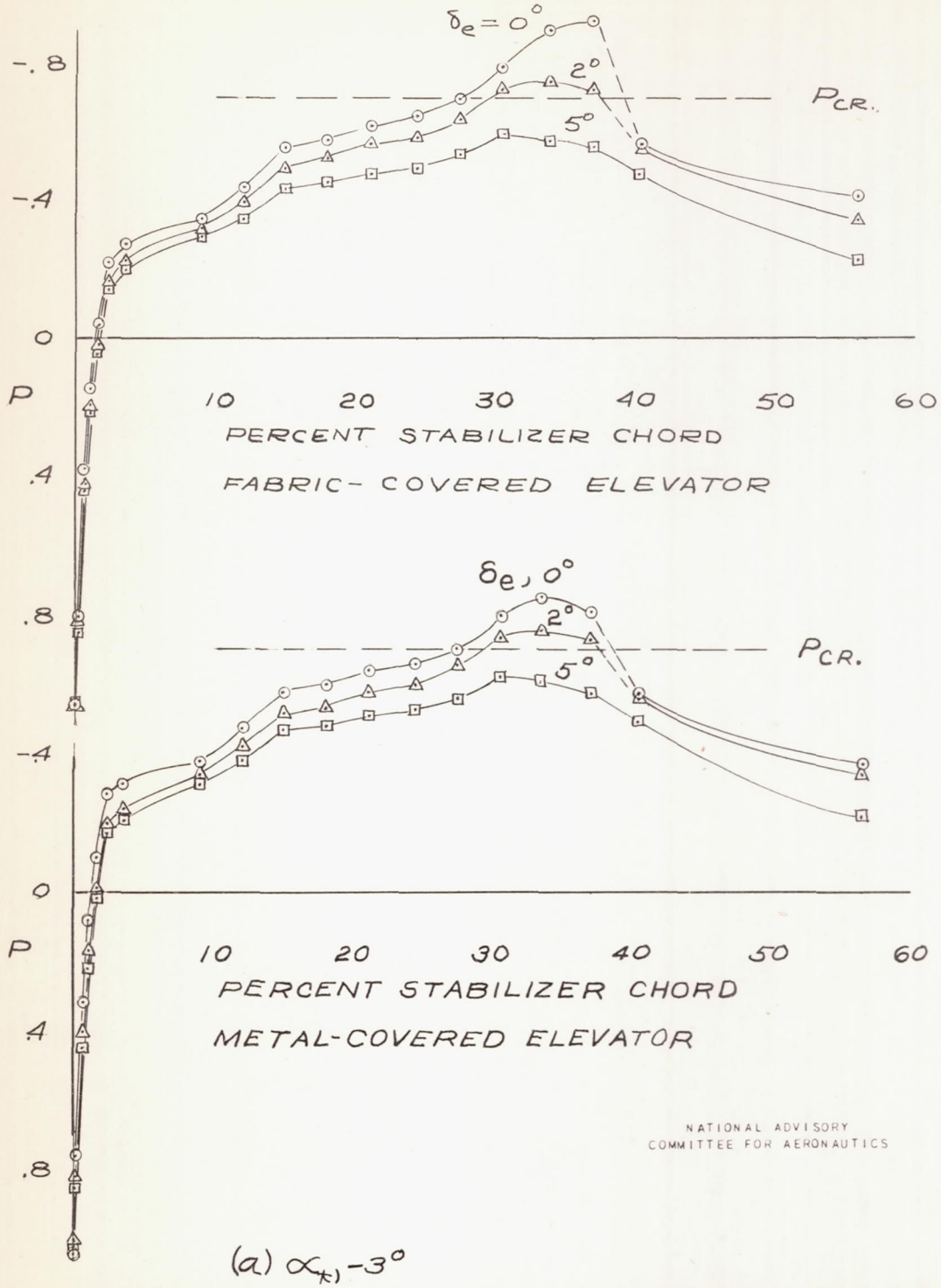

(a) α_t, -3°

FIGURE 21.-VARIATION OF PRESSURE COEFFICIENT WITH CHORDWISE STATION ON THE LOWER SURFACE. M, 0.72; δ_t, 0°; STATION 92.

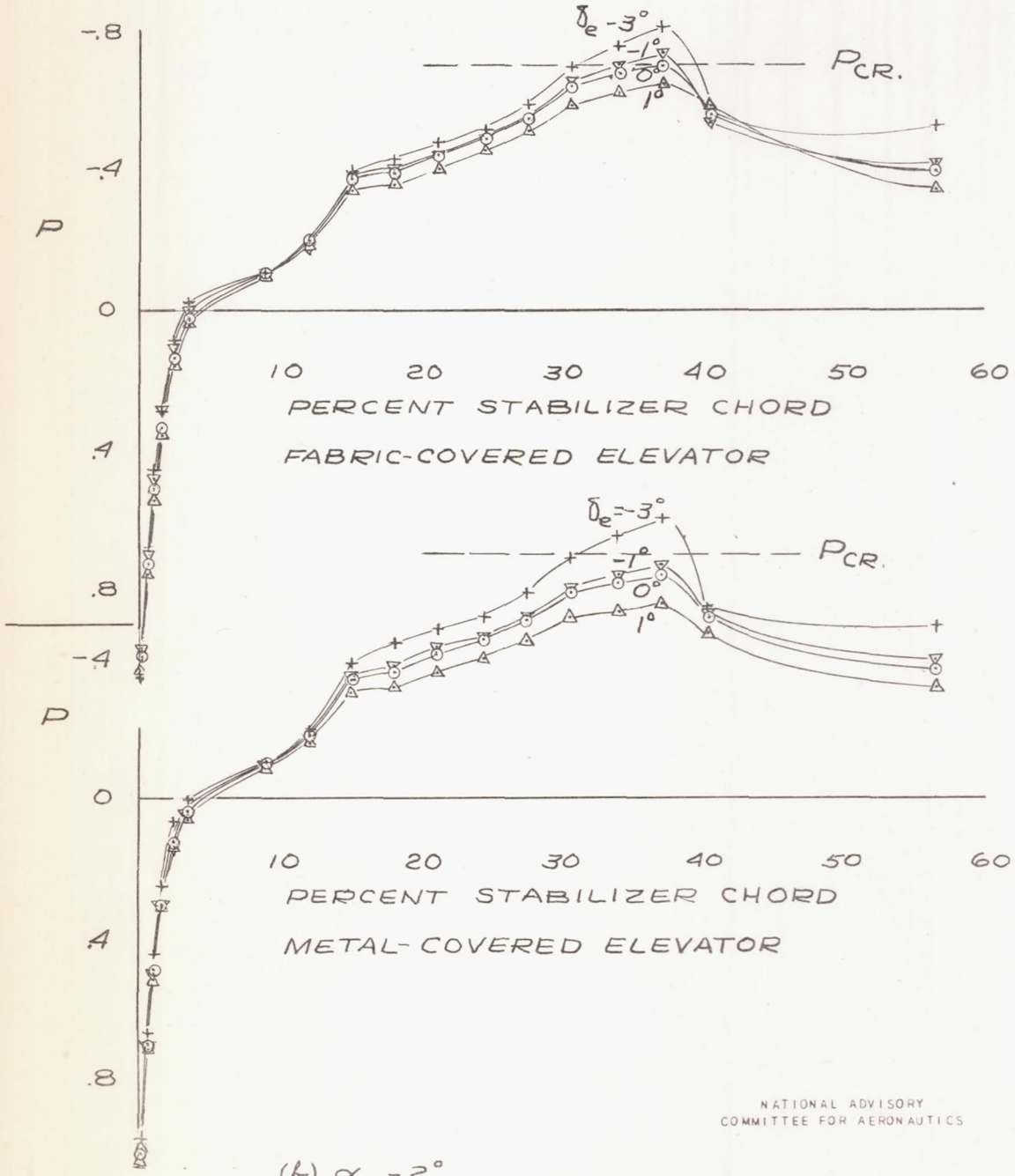

(b) α_t -2°

FIGURE 21.- CONCLUDED.

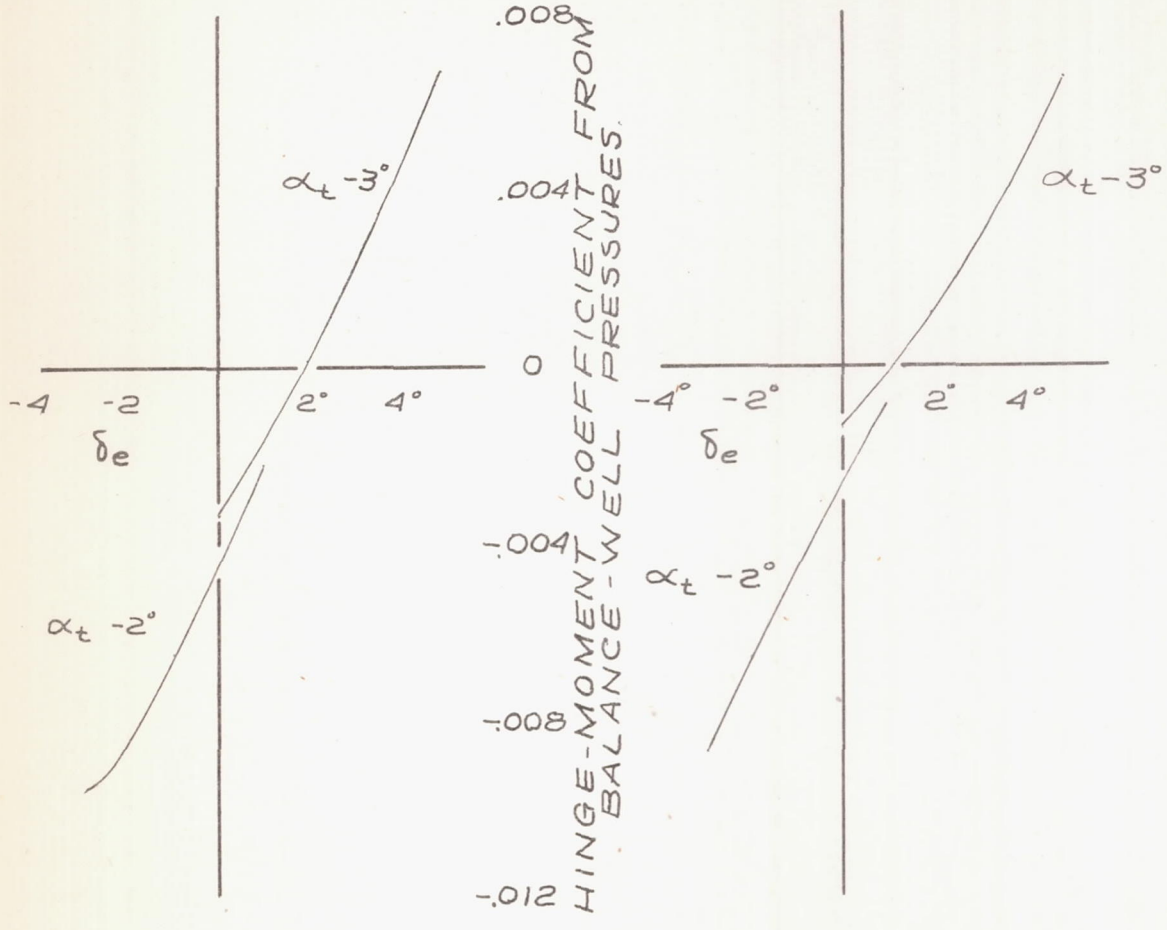

NATIONAL ADVISORY
COMMITTEE FOR AERONAUTICS

FIGURE 22.-VARIATION OF BALANCING HINGE-MOMENT COEFFICIENT WITH ELEVATOR ANGLE. M, 0.72; δ_t, 0°.

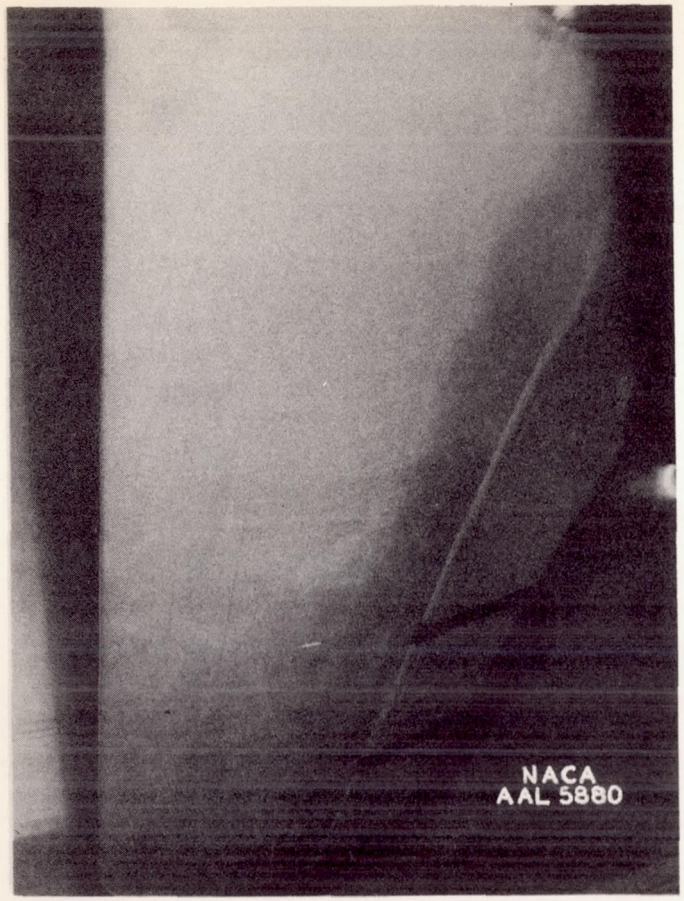

(a) Upper surface.

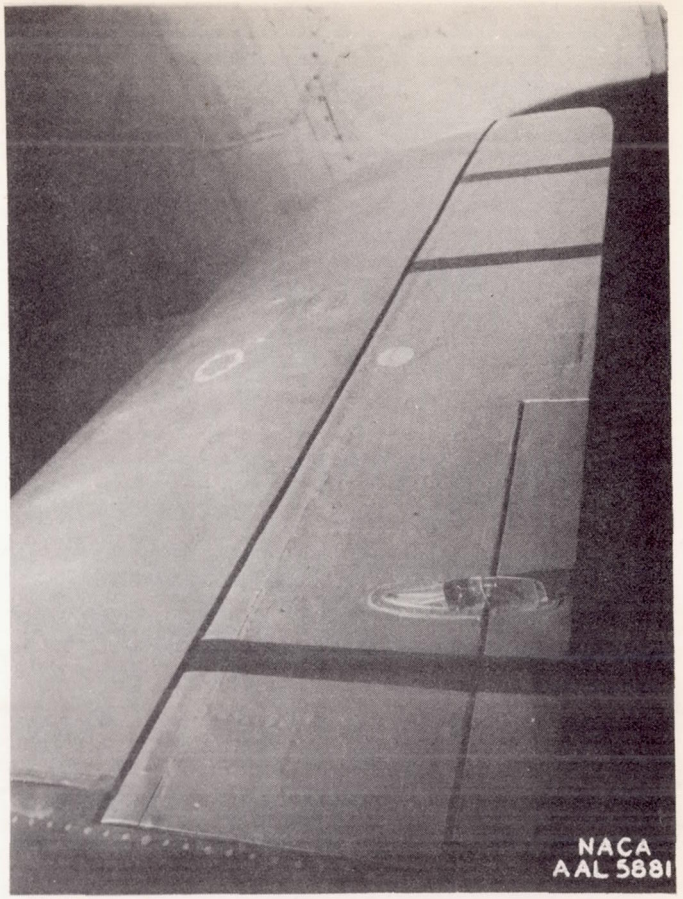

(b) Lower surface.

Figure 23.- The static condition of the bomber stabilizer and fabric-covered elevator before running at high speed.

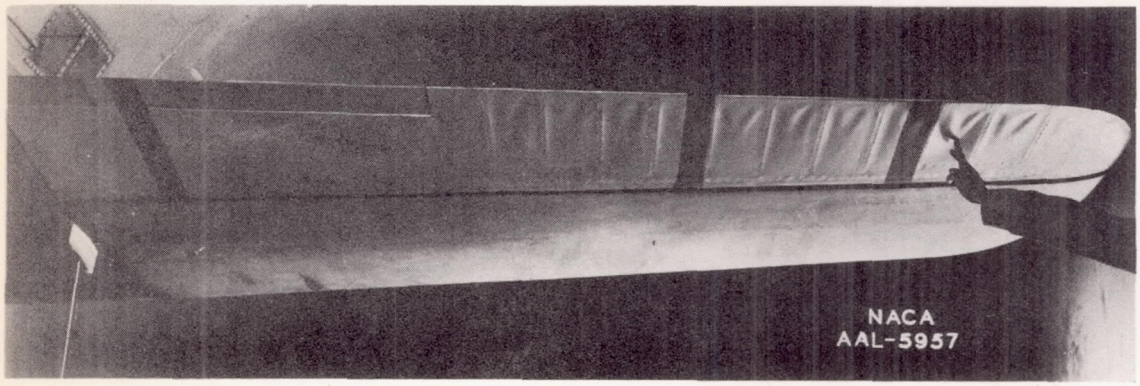

Figure 24.- The static condition of the bomber stabilizer and fabric-covered elevator, after running at high speed.

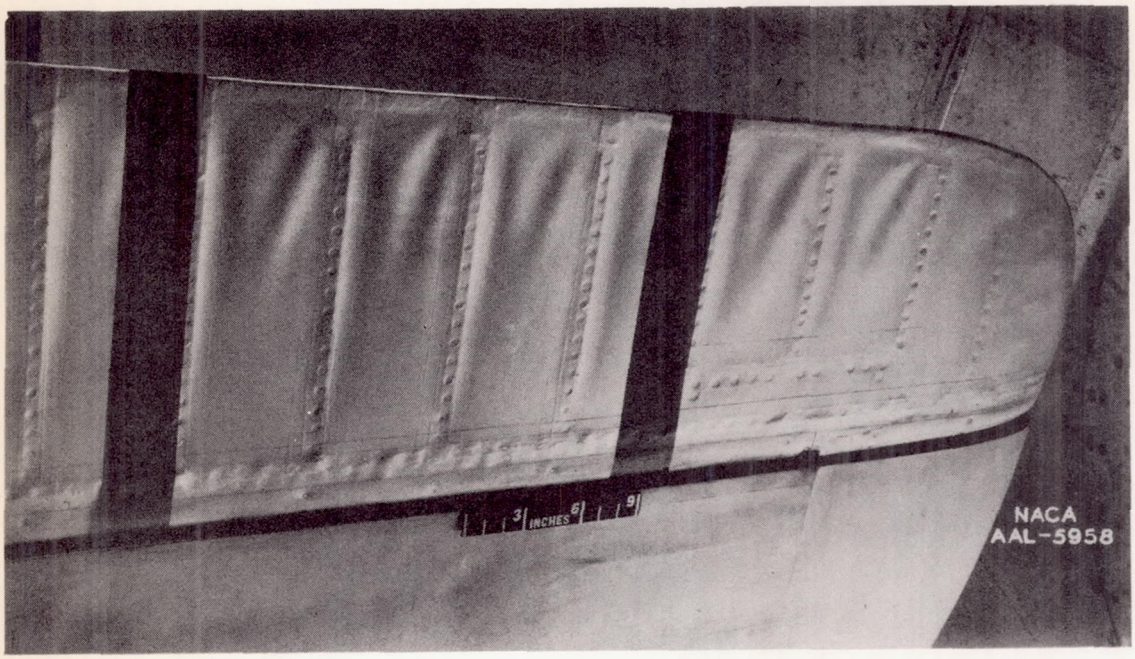

Figure 25.- The static condition of the bomber fabric-covered elevator, after running at high speed.

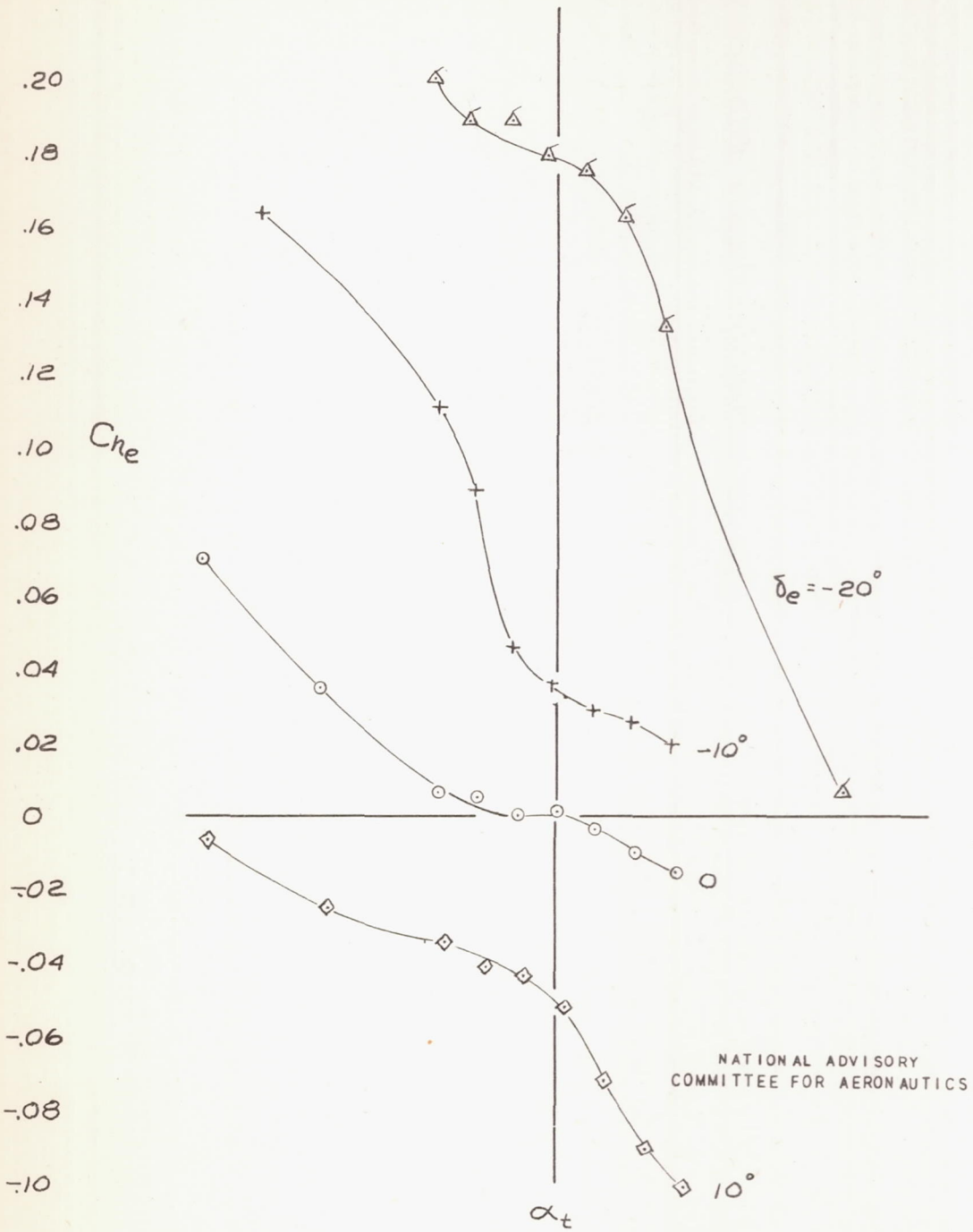

FIGURE 26.- VARIATION OF HINGE-MOMENT COEFFICIENT WITH TAIL ANGLE OF ATTACK FOR THE FABRIC-COVERED ELEVATOR WITH LEAKS IN BALANCE SEAL. M, 0.133; δ_t, 0°.

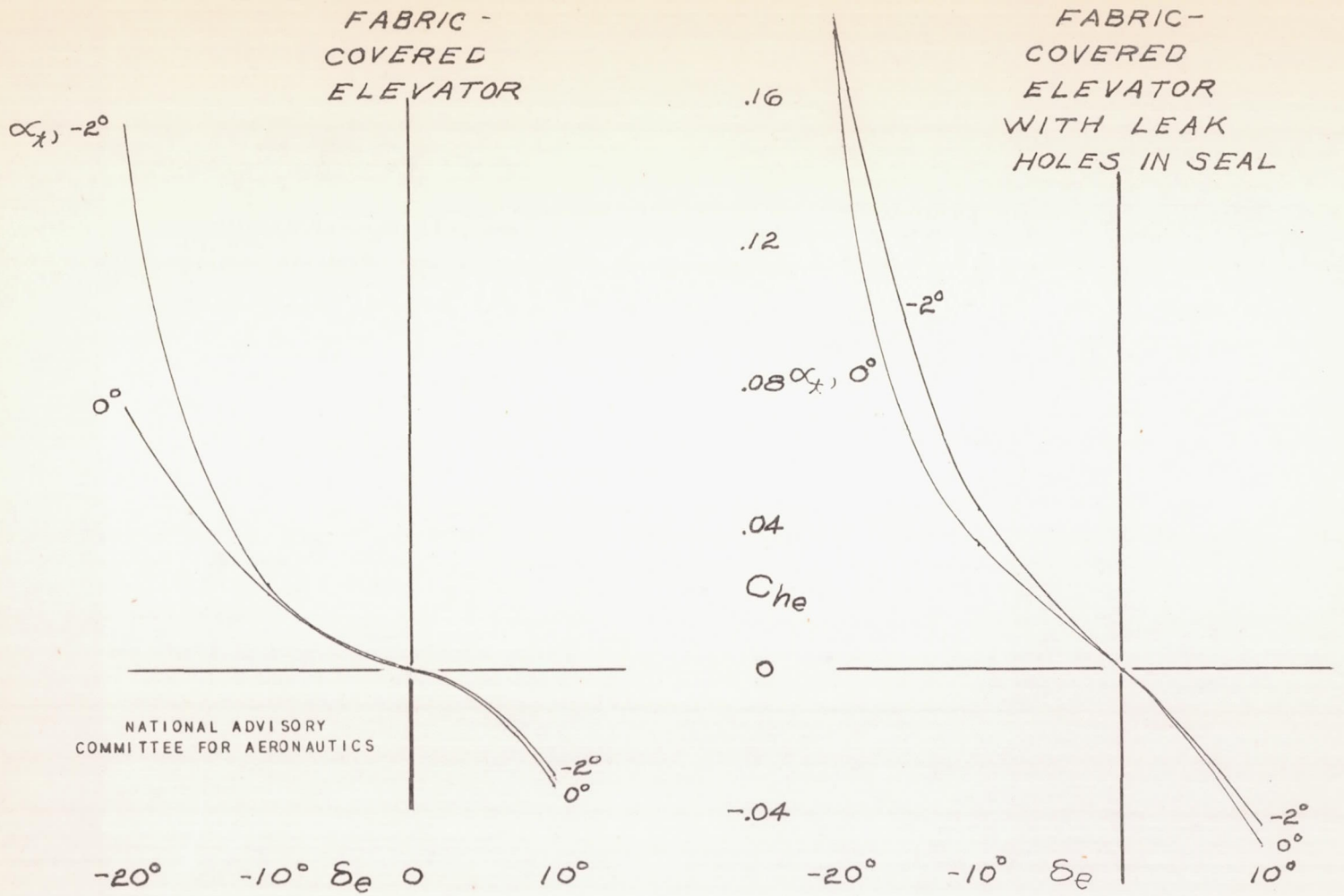

FIGURE 27.-VARIATION OF ELEVATOR HINGE-MOMENT COEFFICIENT WITH ELEVATOR ANGLE; FABRIC WITH AND WITHOUT LEAK HOLES IN THE SEAL; M, 0.133; δ_t, 0°.

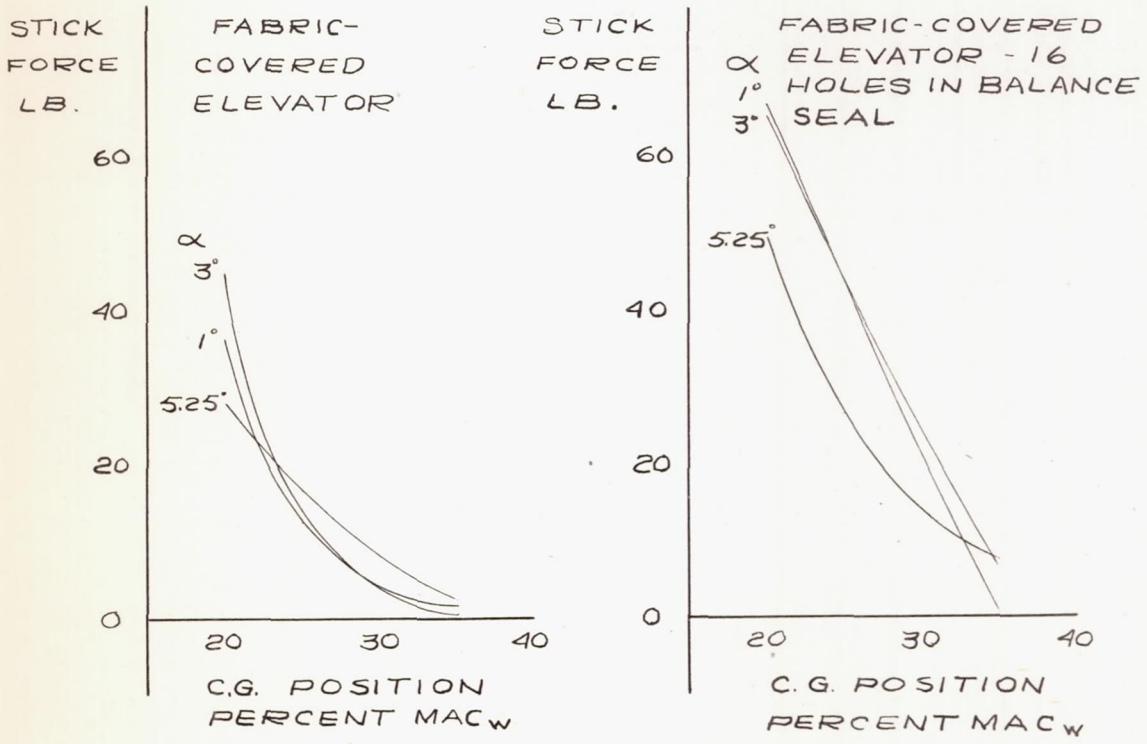

NATIONAL ADVISORY COMMITTEE FOR AERONAUTICS

FIGURE 28.- VARIATION OF ELEVATOR STICK FORCE WITH C.G. POSITION LANDING WITH FLAPS DOWN WITH AND WITHOUT LEAK HOLES IN BALANCE SEAL. M_1 0.133; δ_{t_1} 0.

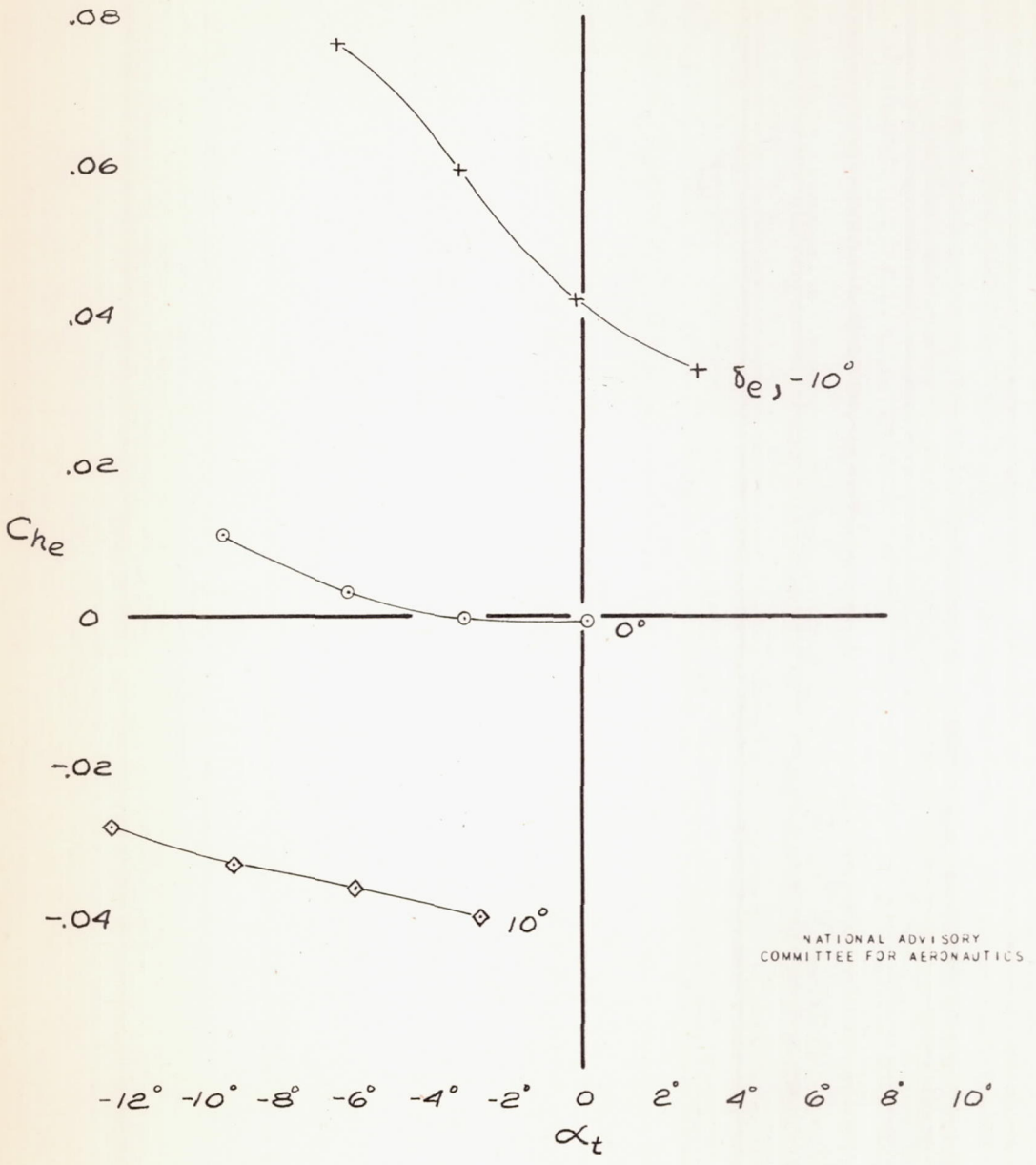

FIGURE 29.- VARIATION OF HINGE-MOMENT COEFFICIENT WITH TAIL ANGLE OF ATTACK, FABRIC-COVERED ELEVATOR WITH LEAK HOLES IN BALANCE SEAL. M, 0.33 ; δ_t, 0°.

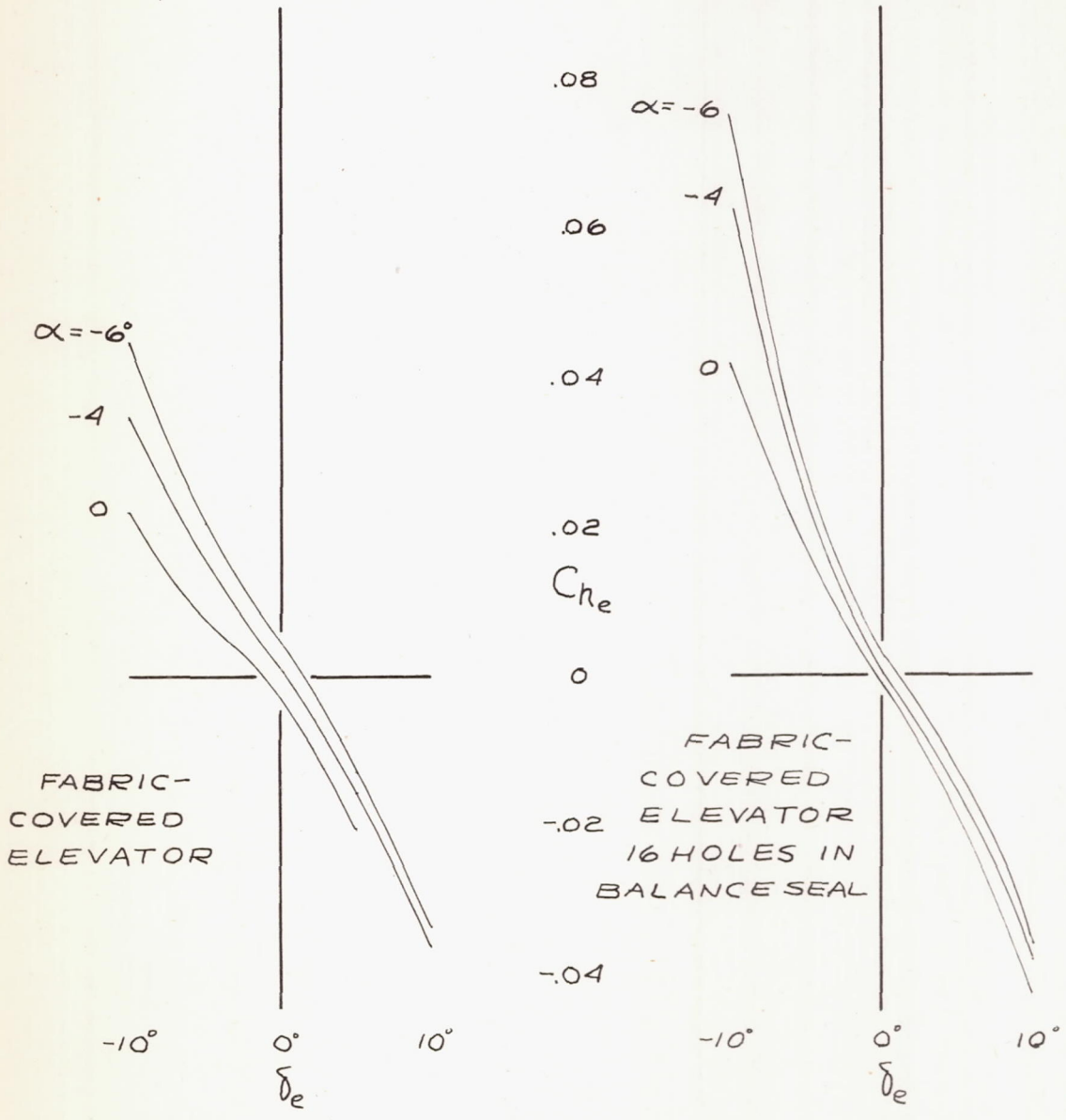

FIGURE 30.- VARIATION OF ELEVATOR HINGE-MOMENT COEFFICIENT WITH ELEVATOR ANGLE, WITH AND WITHOUT HOLES IN THE SEAL. M, 0.33; δ_t, 0°.

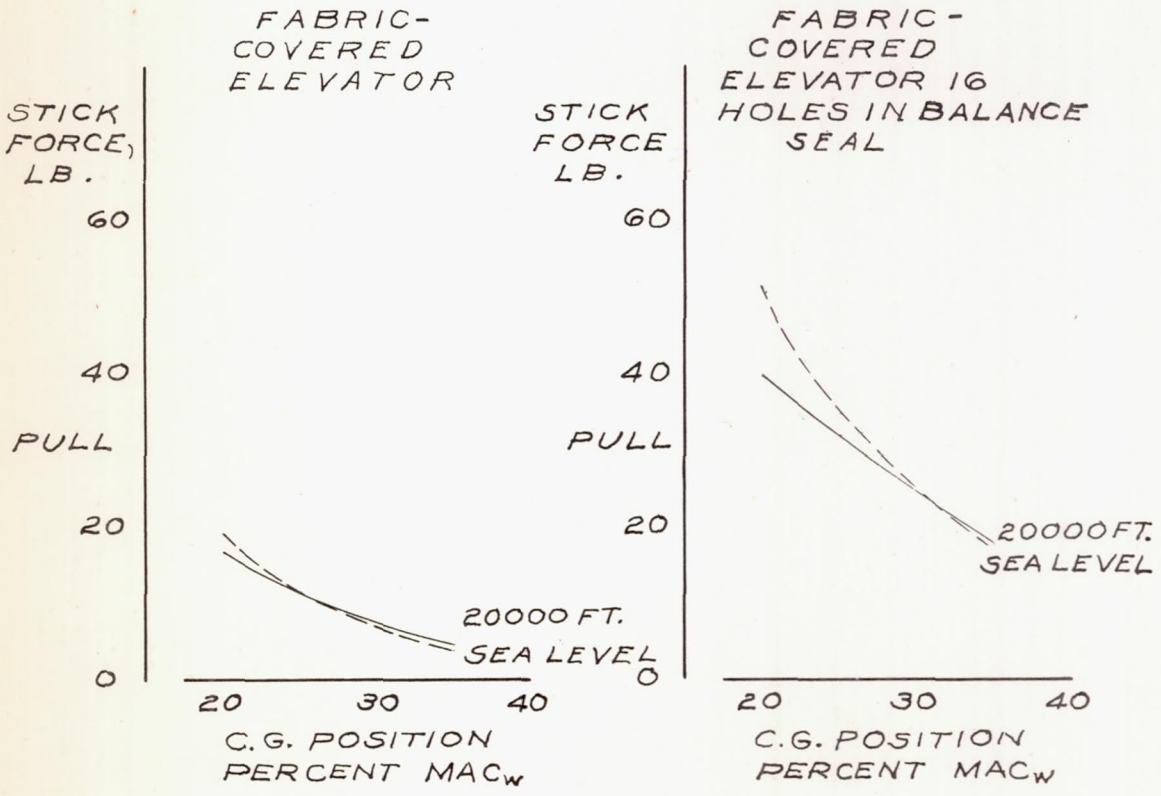

NATIONAL ADVISORY
COMMITTEE FOR AERONAUTICS

FIGURE 31.-VARIATION OF ELEVATOR STICK FORCE WITH C.G. POSITION, WITH AND WITHOUT LEAK HOLES IN SEAL; WEIGHT 25000 LB.; LEVEL FLIGHT; M, 0.33; δ_t, 0°

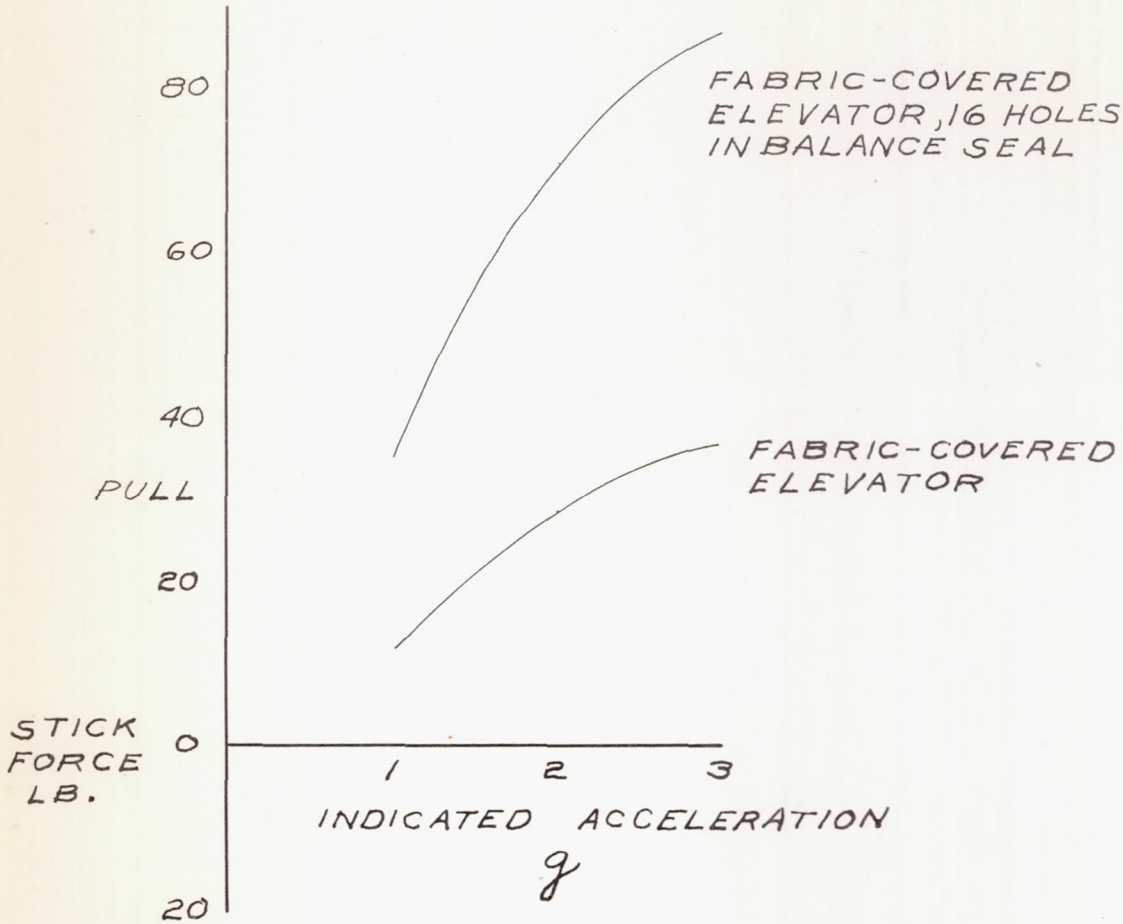

FIGURE 32.-VARIATION OF ELEVATOR STICK FORCE WITH ACCELERATION AT SEA LEVEL, EFFECT OF LEAK HOLES IN BALANCE SEAL; WEIGHT 25000 LB.; C.G. AT 25% M.A.C.; M, 0.33; δ_t, 0°.

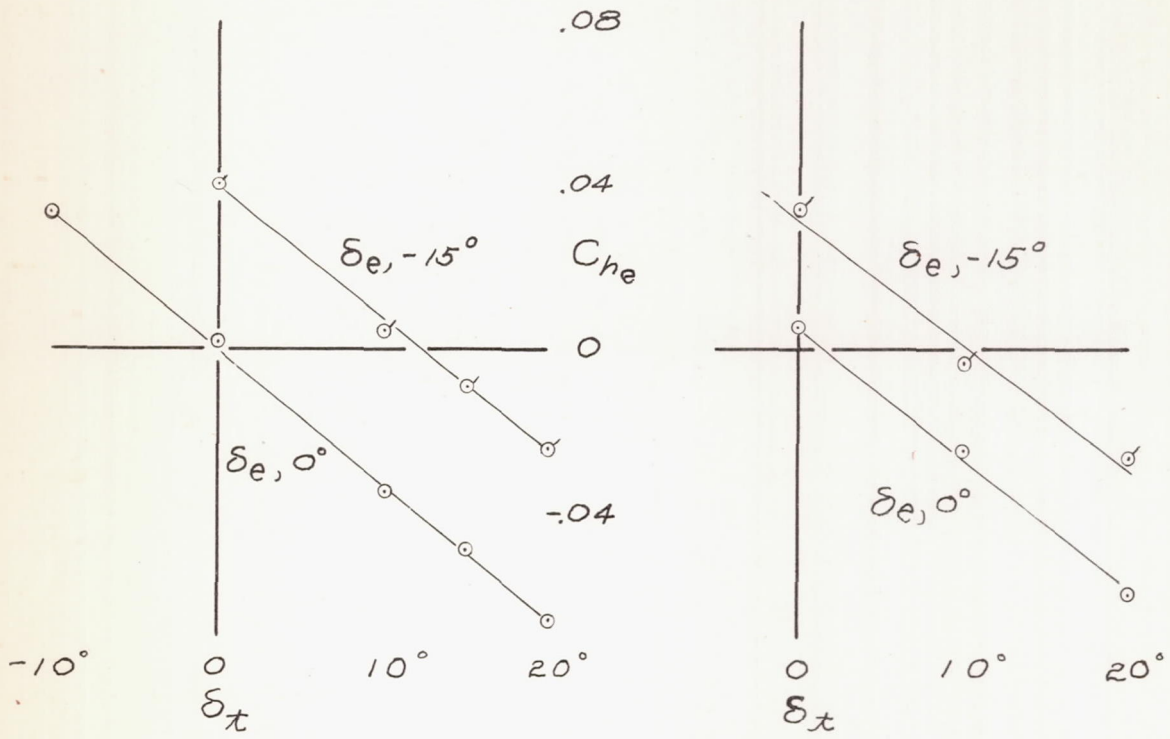

NATIONAL ADVISORY
COMMITTEE FOR AERONAUTICS

FIGURE 33.- VARIATION OF ELEVATOR HINGE-MOMENT COEFFICIENT WITH TAB ANGLE. M, 0.133; α_t 0°.

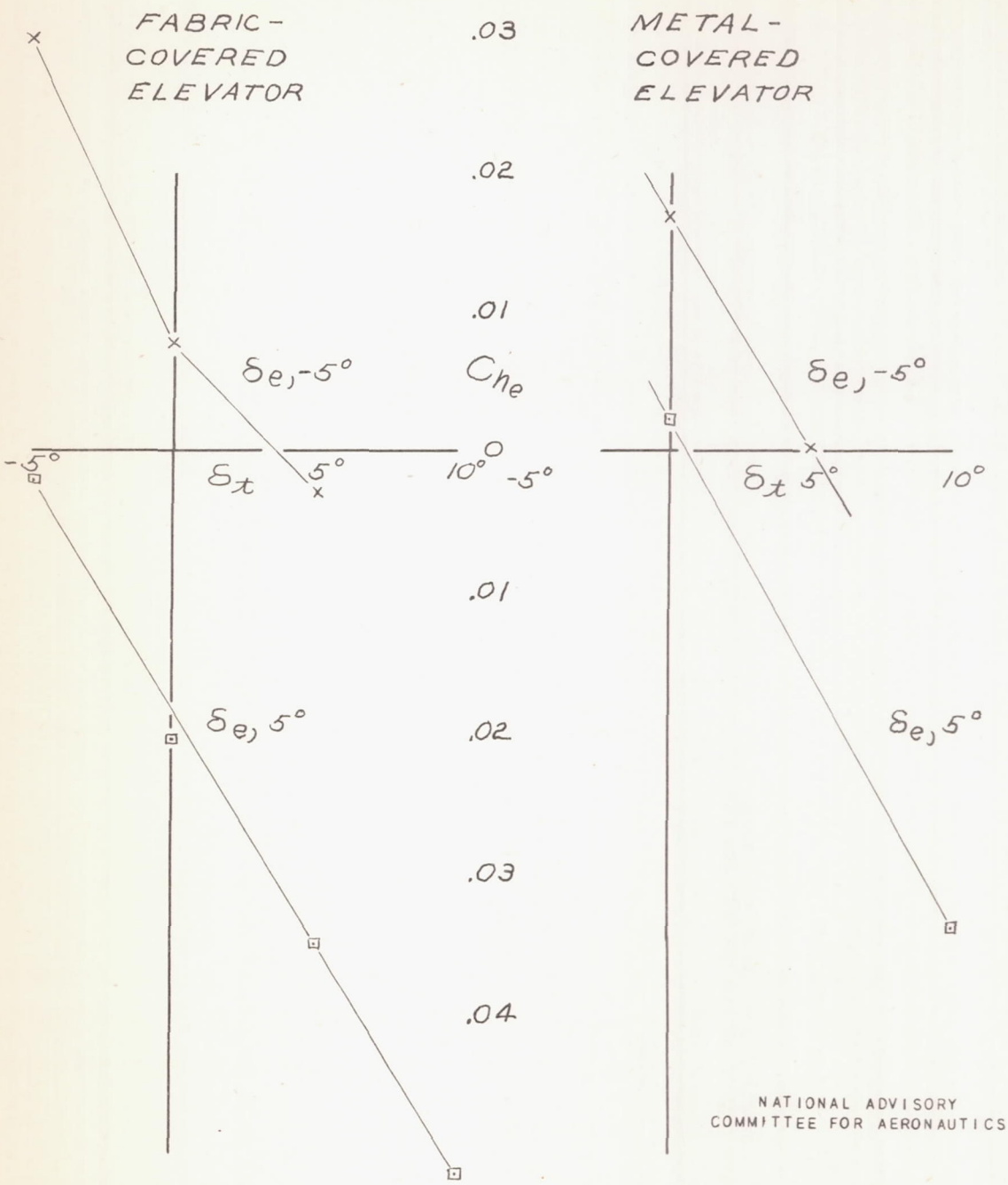

FIGURE 34.-VARIATION OF ELEVATOR HINGE-MOMENT COEFFICIENT WITH TAB ANGLE. M, 0.33; α_t, 0°;

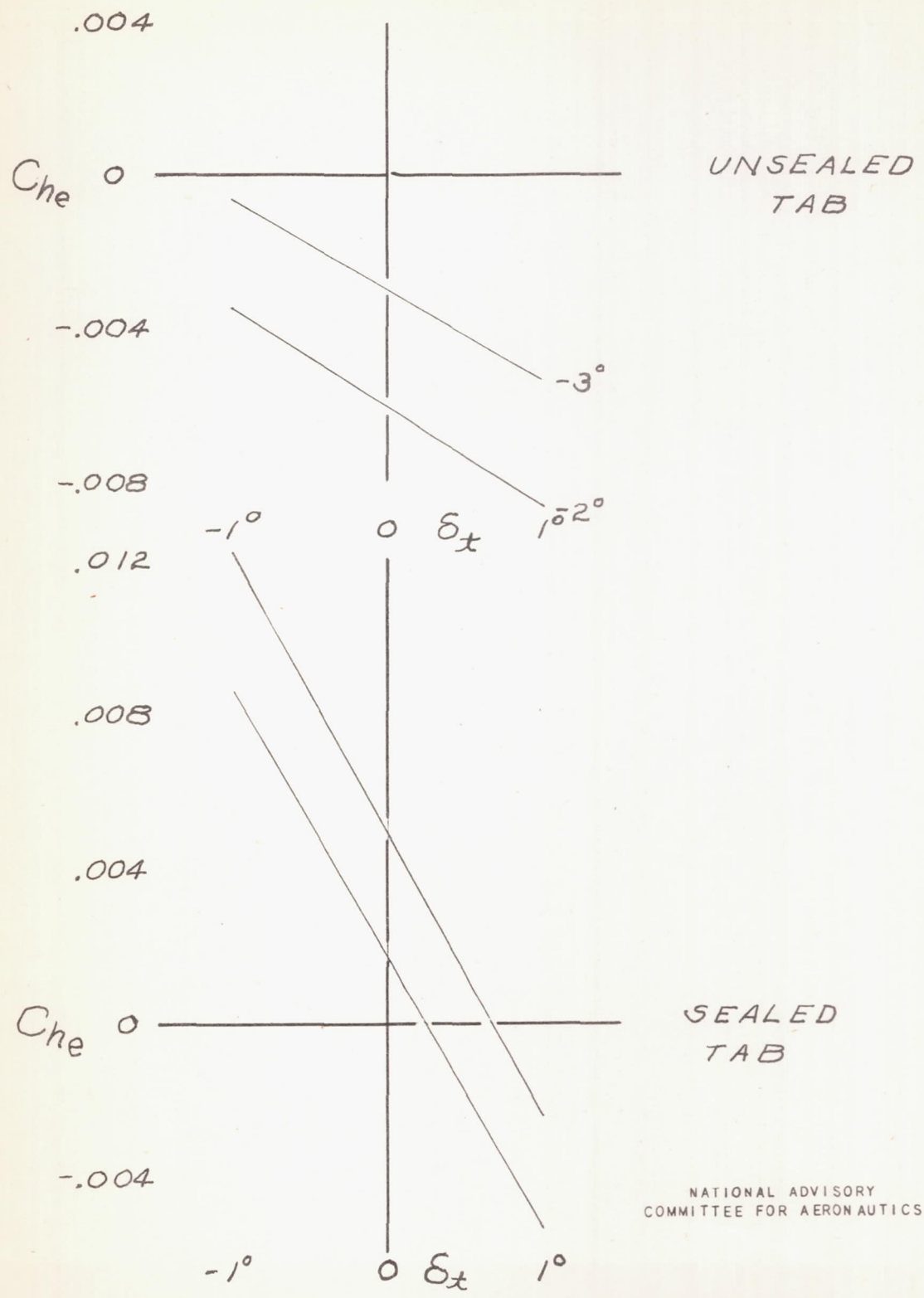

FIGURE 35.- VARIATION OF ELEVATOR HINGE-MOMENT COEFFICIENT WITH TAB ANGLE. M, 0.72; α_t, 0°.

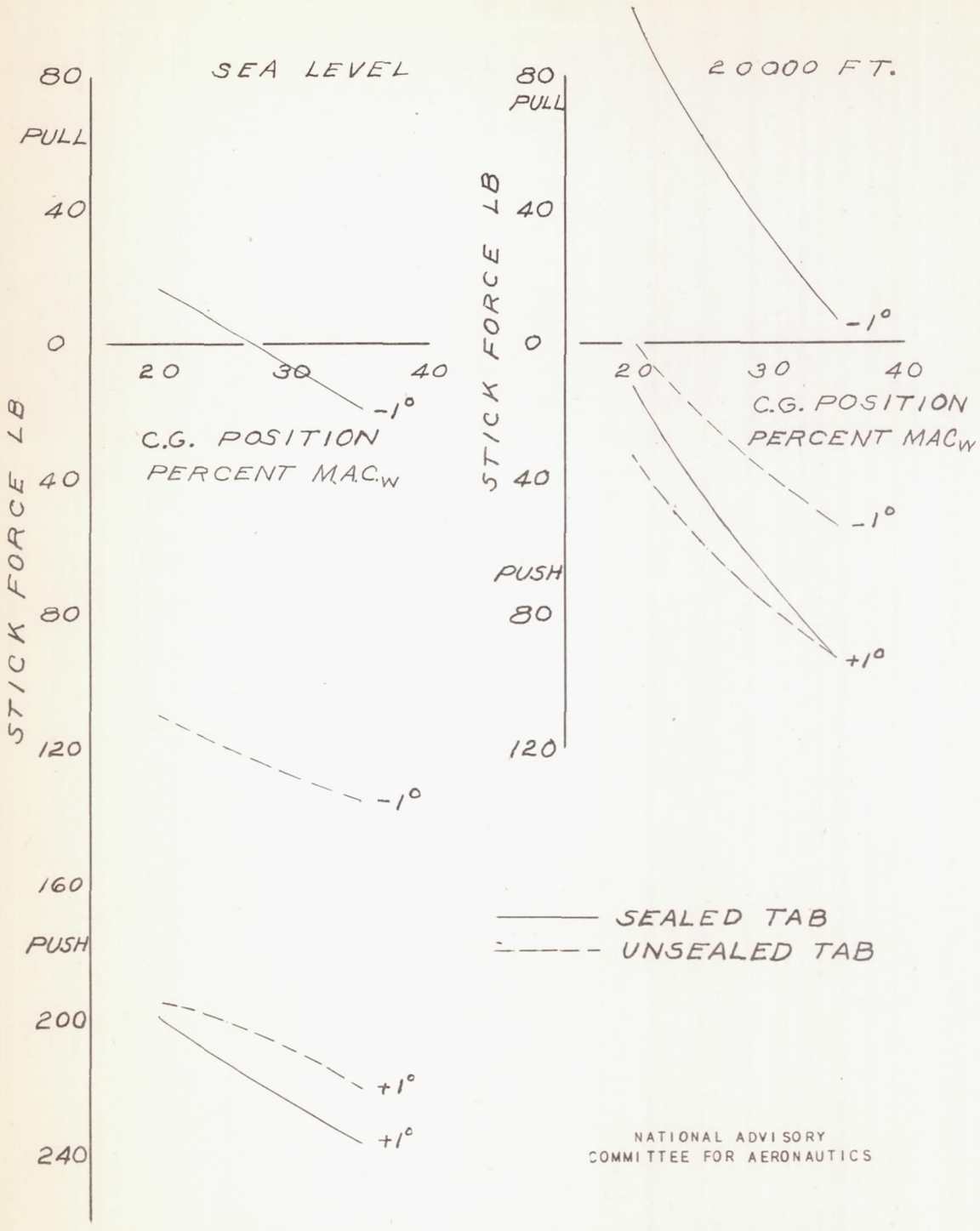

FIGURE 36.-VARIATION OF STICK FORCE WITH C.G. POSITION FOR THE SEALED AND UNSEALED TAB; WEIGHT 25000LB; M, 0.72.

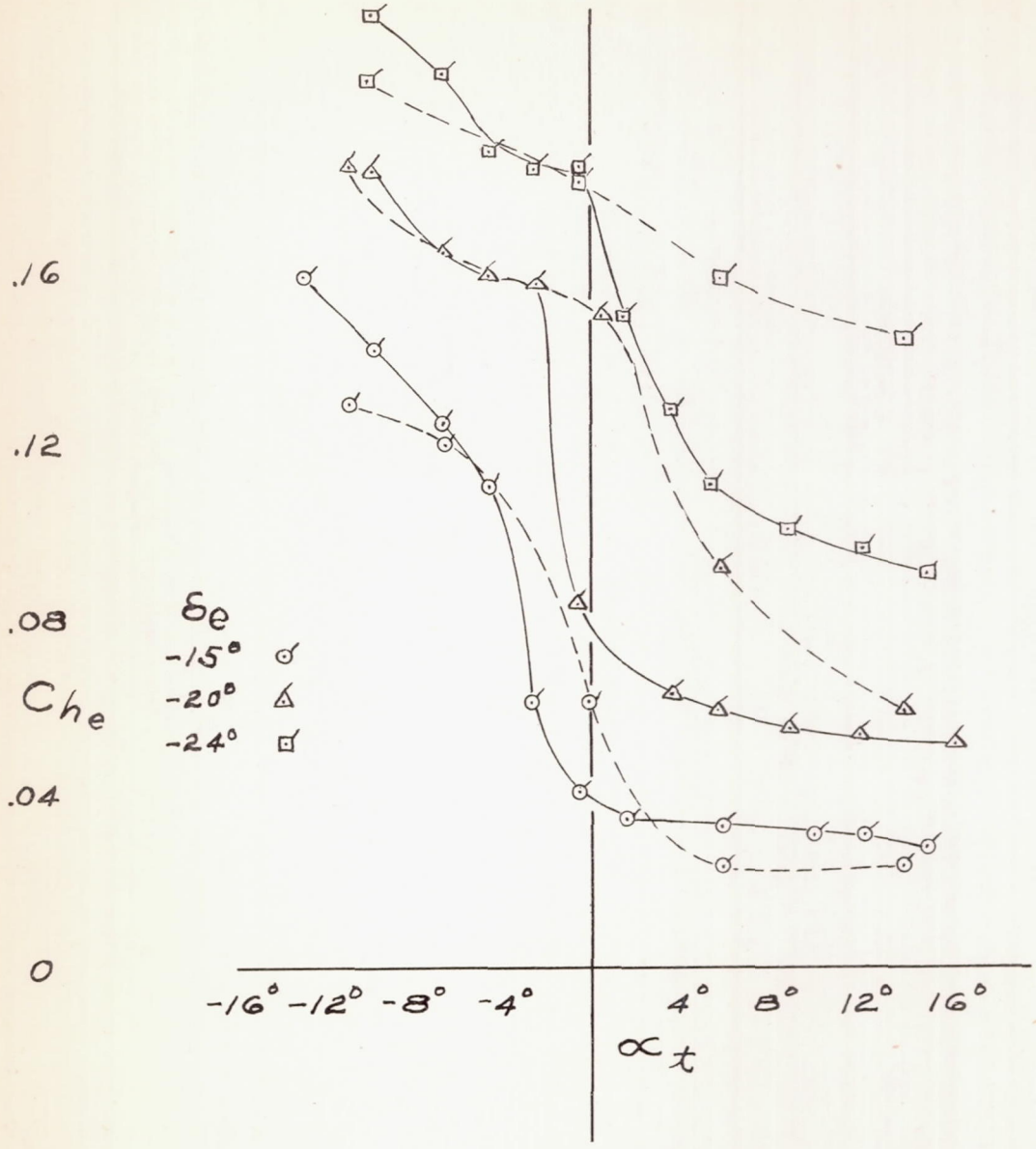

-------TRANSITION FIXED AT 20% CHORD
———SMOOTH HORIZONTAL TAIL SURFACE

NATIONAL ADVISORY
COMMITTEE FOR AERONAUTICS

FIGURE 37.—VARIATION OF HINGE-MOMENT COEFFICIENT WITH TAIL ANGLE OF ATTACK FOR THE FABRIC-COVERED ELEVATOR WITH AND WITHOUT TRANSITION FIXED. M, 0.133; $\delta_t = 0°$.

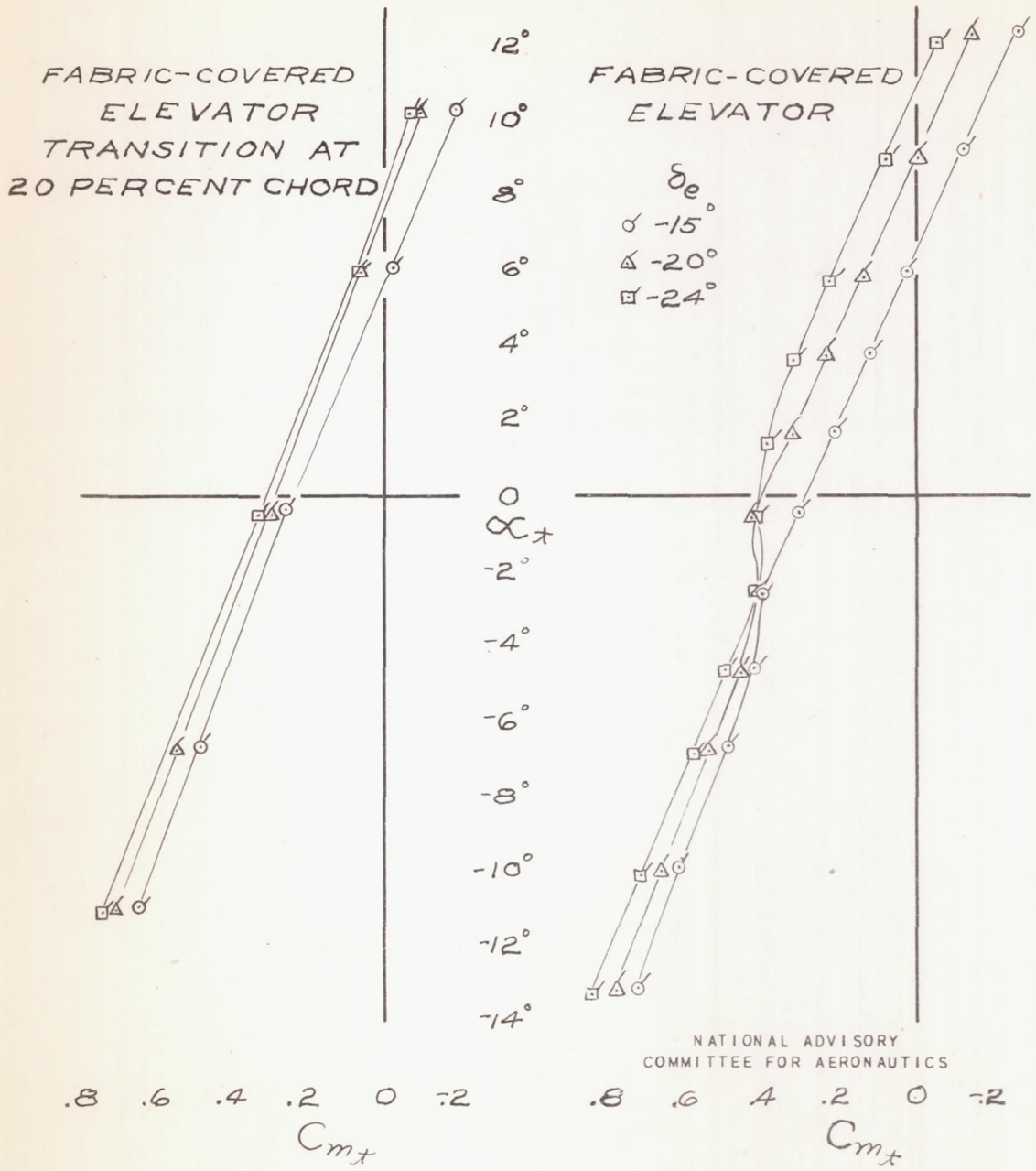

FIGURE 38.- VARIATION OF PITCHING-MOMENT COEFFICIENT DUE TO THE TAIL WITH TAIL ANGLE OF ATTACK, WITH AND WITHOUT TRANSITION FIXED; M, 0.133; δ_t, 0°.

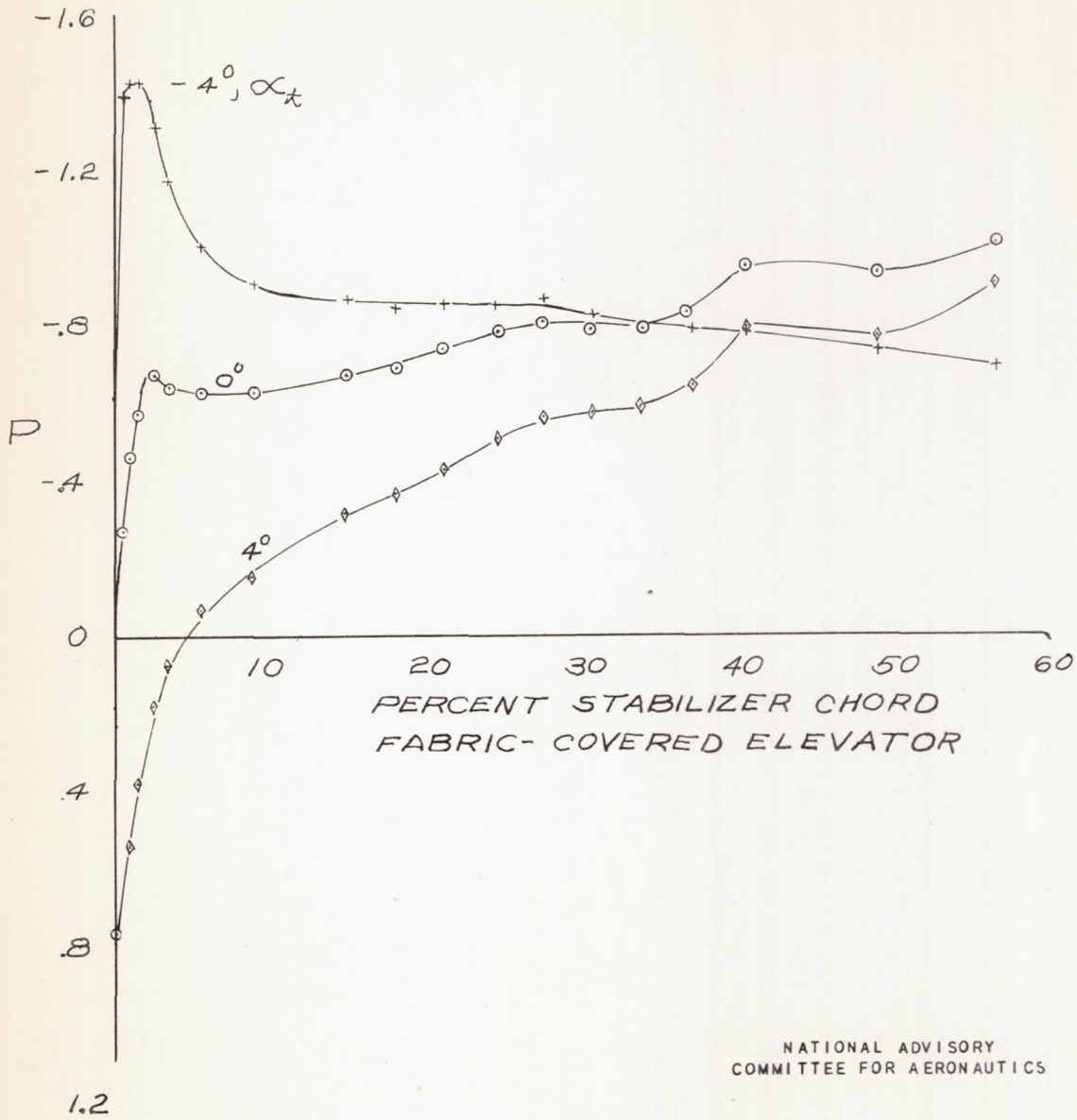

FIGURE 39.- VARIATION OF PRESSURE DISTRIBUTION OVER THE HORIZONTAL STABILIZER WITH TAIL ANGLE OF ATTACK; M, 0.133; δ_e, -20°; δ_t, 0°.

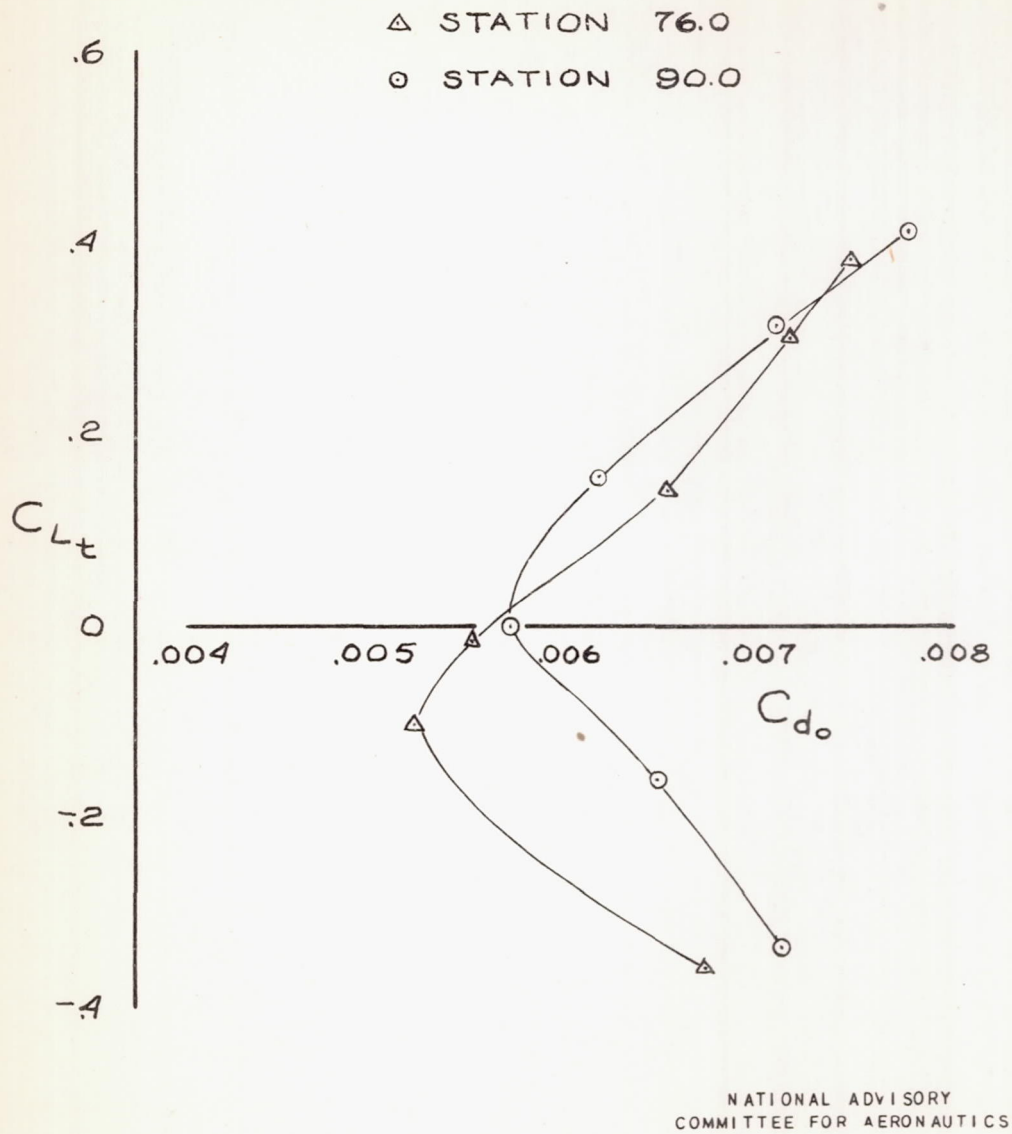

FIGURE 40.- VARIATION OF SECTION DRAG COEFFICIENT WITH LIFT COEFFICIENT; BOMBER STABILIZER WITH FABRIC-COVERED ELEVATOR; M, 0.33; δ_e, 0°; δ_t, 0°.

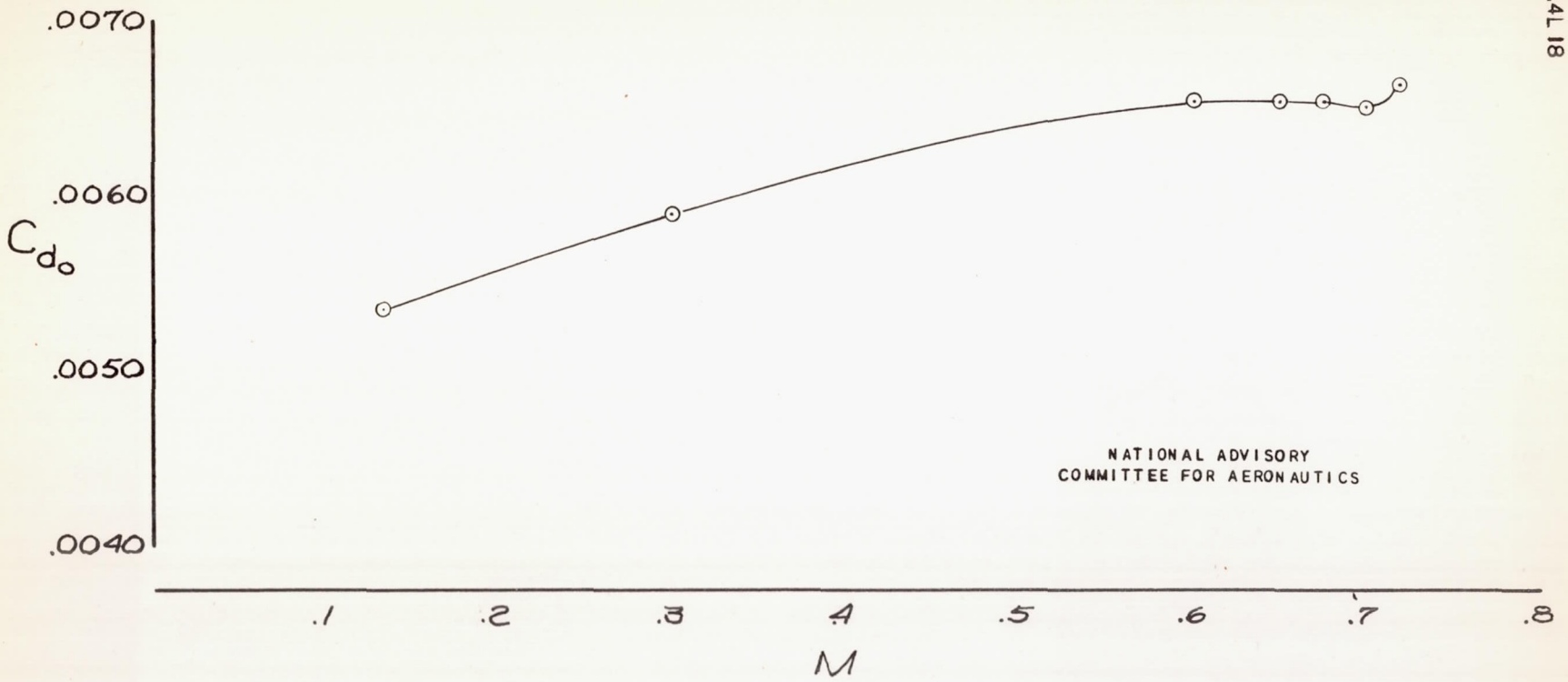

FIGURE 41. - VARIATION OF SECTION DRAG COEFFICIENT WITH MACH NUMBER, BOMBER STABILIZER WITH FABRIC-COVERED ELEVATOR; STATION 83.5; $\delta_e = 0°$; $\delta_t = 0°$.